

APPENDIX B

Equations of State for Mixtures of R-32, R-125, R-134a, R-143a, and R-152a

[manuscript to be submitted to the *Journal of Physical and Chemical Reference Data*]

Equations of State for Mixtures of R-32, R-125, R-134a, R-143a, and R-152a

Eric W. Lemmon¹

Physical and Chemical Properties Division, National Institute of Standards and Technology, 325 Broadway, Boulder, Colorado 80305

Richard T Jacobsen

Idaho National Engineering and Environmental Laboratory, Idaho Falls, Idaho 83415-3790

Mixture models explicit in Helmholtz energy have been developed to calculate the thermodynamic properties of refrigerant mixtures containing R-32, R-125, R-134a, R143a, and R-152a. The Helmholtz energy of the mixture is the sum of the ideal gas contribution, the compressibility (or real gas) contribution, and the contribution from mixing. The independent variables are the density, temperature, and composition. The model may be used to calculate thermodynamic properties of mixtures, including dew and bubble point properties and critical points, within the experimental uncertainties of the available measured properties. It incorporates the most accurate equations of state available for each pure fluid. The estimated uncertainties of calculated properties are 0.1% in density and 0.5% in heat capacities and the speed of sound. Calculated bubble point pressures are generally accurate to within 0.5%.

Key words: density, equation of state; refrigerant mixtures; R-32; R-125; R-134a; R-143a; R-152a; speed of sound, thermodynamic properties.

¹ Electronic mail: ericl@boulder.nist.gov

Contents

List of Symbols	5
Introduction	7
The Mixture Equation	8
Vapor-Liquid Equilibrium (VLE) Properties	12
Comparisons to Data	13
The R-32/125 System.....	14
The R-32/134a System	16
The R-125/134a, R-125/143a, R-134a/143a, and R-134a/152a Systems.....	16
The Ternary Mixtures.....	18
Other thermodynamic properties.....	19
Accuracy Assessment.....	19
Acknowledgments	20
References	20

List of Tables

Table 1. Pure fluid equations of state for the refrigerants used in the mixture model	23
Table 2. Coefficients and exponents of the mixture equations	23
Table 3. Parameters of the mixture equations	23
Table 4. Summary comparisons of mixture properties calculated from the model to refrigerant mixture data.....	24

List of Figures

1.	Comparisons of densities calculated with the mixture model to experimental data for the R-32/125 binary mixture.	30
2.	Comparisons of bubble point pressures calculated with the mixture model to experimental data for the R-32/125 binary mixture.	32
3.	Comparisons of densities calculated with the mixture model to experimental data for the R-32/134a binary mixture.	33
4.	Comparisons of bubble point pressures calculated with the mixture model to experimental data for the R-32/134a binary mixture.	35
5.	Comparisons of densities calculated with the mixture model to experimental data for the R-125/134a binary mixture.	36
6.	Comparisons of densities calculated with the mixture model to experimental data for the R-125/143a binary mixture.	37
7.	Comparisons of densities calculated with the mixture model to experimental data for the R-134a/143a binary mixture.	38
8.	Comparisons of densities calculated with the mixture model to experimental data for the R-134a/152a binary mixture.	39
9.	Comparisons of bubble point pressures calculated with the mixture model to experimental data for the R-125/134a, R-125/143a, R-134a/143a, and R-134a/152a binary mixtures.	40
10.	Comparisons of densities calculated with the mixture model to experimental data for the R-32/125/134a ternary mixture.	41
11.	Comparisons of bubble point pressures calculated with the mixture model to experimental data for the R-32/125/134a and R-125/134a/143a ternary mixtures.	43
12.	Comparisons of densities calculated with the mixture model to experimental data for the R-125/134a/143a ternary mixture.	44
13.	Comparisons of isochoric heat capacities calculated with the mixture model to experimental data for the R-32/125, R-32/134a, R-125/134a, and R-125/143a binary mixtures.	45
14.	Comparisons of isochoric heat capacities calculated with the mixture model to experimental data for the R-32/125/134a ternary mixture.	46
15.	Comparisons of the speed of sound in the vapor phase calculated with the mixture model to experimental data for the R-32/125, R-32/134a, R-125/134a, and R-125/143a binary mixtures.	47
16.	Comparisons of the speed of sound in the vapor phase calculated with the mixture model to experimental data for the R-32/125/134a ternary mixture.	48
17.	Comparisons of the speed of sound in the liquid phase calculated with the mixture model to experimental data for the R-134a/152a binary mixture.	49

List of Symbols

<u>Symbol</u>	<u>Physical quantity</u>	<u>Unit</u>
a	Helmholtz energy	J/mol
A	Helmholtz energy	J
c_p	Isobaric heat capacity	J/(mol · K)
c_v	Isochoric heat capacity	J/(mol · K)
d	Density exponent	
f	fugacity	MPa
F	Generalized factor	
g	Gibbs energy	J/mol
h	Enthalpy	J/mol
l	Density exponent	
m	Number of components	
M	Molar mass	g/mol
n	Number of moles	mol
p	Pressure	MPa
R	Molar gas constant	J/(mol · K)
s	Entropy	J/(mol · K)
t	Temperature exponent	
T	Temperature	K
u	Internal energy	J/mol
v	Molar volume	dm ³ /mol
V	Volume	dm ³
w	Speed of sound	m/s
x	Composition	mole fraction
Z	Compressibility factor ($Z = p/\rho RT$)	
α	Reduced Helmholtz energy ($\alpha = a/RT$)	
δ	Reduced density ($\delta = \rho/\rho_c$)	
ρ	Molar density	mol/dm ³

τ	Inverse reduced temperature ($\tau = T_c/T$)	
μ	Chemical potential	J/mol
ξ	Reduced density parameter	dm ³ /mol
ζ	Reduced temperature parameter	K

Superscripts

0	Ideal gas property
E	Excess property
$idmix$	Ideal mixture
r	Residual
'	Saturated liquid state
"	Saturated vapor state

Subscripts

0	Reference state property
c	Critical point property
calc	Calculated using an equation
data	Experimental value
i, j	Property of component i or j
red	Reducing parameter
σ	Saturation property

Introduction

The need for equations of state capable of accurate prediction of thermodynamic properties of environmentally-safe fluids continues as new applications are developed requiring the use of refrigerant mixtures. These mixtures of refrigerants are used as environmentally acceptable replacements for chlorofluorocarbons and hydrochlorofluorocarbons in refrigeration, heat pumps, foam-blown, and other applications. Mixture equations are required to evaluate the performance of possible working fluids.

A model is presented here for calculating the thermodynamic properties of refrigerant mixtures which replaces the model reported by Lemmon and Jacobsen (1999). This model was initially reported by Lemmon (1996) and general details and comparisons among different implementations of the model were reported by Lemmon and Tillner-Roth (1999). The model may be used to calculate all thermodynamic properties of mixtures at various compositions, including dew and bubble-point properties and critical points. The mixture model is similar to the model presented by Tillner-Roth *et al.* (1998) and published by the Japan Society of Refrigerating and Air Conditioning Engineers (JSRAE). However, the work presented here uses generalized equations for several of the mixtures, whereas separate equations for each binary mixture were developed in the JSRAE equations.

The mixture model presented here is based on corresponding states theory and uses reducing parameters which are dependent on the mole fractions of the mixture constituents and critical points of the pure fluids to modify absolute values of the mixture density and temperature. This approach allows the thermodynamic properties of the mixture to be based largely on the contributions from the pure fluids. Without additional mixing functions, the model is similar to that for an ideal mixture, and only the excess values, or the departures from ideality, are required to accurately model the properties of the mixture.

The model uses the Helmholtz energy as the basis for all calculations. The Helmholtz energy is one of four fundamental properties from which all other thermodynamic properties can be calculated using simple derivatives. The Helmholtz energy of the mixture is calculated as the sum of an ideal gas contribution, a real fluid contribution, and a contribution from mixing. The Helmholtz energy from the contributions of the ideal gas and the real fluid behavior is determined at the reduced density and temperature of the mixture using accurate pure fluid

equations of state for the mixture components. Reducing parameters, dependent on the mole fractions of the constituents, are used to modify values of density and temperature for the mixture.

The contribution from mixing, a modified excess function, is given by an empirical equation. An excess property of a mixture is defined as the actual mixture property at a given condition minus the value for an ideal solution at the same condition. In most other work dealing with excess properties, the mixing condition is defined at constant pressure and temperature. Because the independent variables for the pure fluid Helmholtz energy equations are reduced density and temperature, properties are calculated here at the reduced density and temperature of the mixture. The shape of the modified excess function is similar for many binary mixtures, and relatively simple scaling factors can be used to determine its magnitude for a particular application. While this approach is arbitrary and different from the usual excess property format, it results in an accurate representation of the single phase properties and phase boundaries for pure fluids and their mixtures.

Three separate models (*i.e.*, three separate excess functions) were developed to calculate the properties of the refrigerant mixtures studied in this work. The first two describe the properties of the binary mixtures R-32/125 and R-32/134a. The shapes of the excess functions for these two mixtures differ from each other and from those of the other mixtures studied in this work, and could not be modeled using a generalized equation. This was first noticed in the work of Lemmon (1996) which required additional terms in the mixing functions for these two binary mixtures. On the other hand, the shapes of the excess functions for the mixtures R-125/134a, R-125/143a, R-134a/143a, and R-134a/152a were similar enough that one function could be developed that described the properties of all these systems. Additionally, experimental data for the ternary mixtures R-32/125/134a and R-125/134a/143a showed that no additional parameters would be required to model these multi-component mixtures.

The Mixture Equation

The equation for the mixture Helmholtz energy used in this work is

$$a = a^{id_{mix}} + a^E. \quad (1)$$

The Helmholtz energy for an ideal mixture as used in this work defined in terms of density and temperature is

$$a^{idmix} = \sum_{i=1}^m x_i [a_i^0(\rho, T) + a_i^r(\delta, \tau) + RT \ln x_i], \quad (2)$$

where ρ and T are the mixture density and temperature, δ and τ are the reduced mixture density and temperature, m is the number of components in the mixture, a_i^0 is the ideal gas Helmholtz energy of component i , a_i^r is the residual Helmholtz energy of component i , and the x_i are the mole fractions of the mixture constituents. References for the pure fluid ideal gas Helmholtz energy and residual Helmholtz energy equations are given in Table 1.

The reduced values of density and temperature for the mixture models used here are

$$\delta = \rho / \rho_{red} \text{ and} \quad (3)$$

$$\tau = T_{red} / T, \quad (4)$$

where ρ and T are the mixture density and temperature, and ρ_{red} and T_{red} are the reducing values,

$$\rho_{red} = \left[\sum_{i=1}^m \frac{x_i}{\rho_{c_i}} + \sum_{i=1}^{m-1} \sum_{j=i+1}^m x_i x_j \xi_{ij} \right]^{-1} \text{ and} \quad (5)$$

$$T_{red} = \sum_{i=1}^m x_i T_{c_i} + \sum_{i=1}^{m-1} \sum_{j=i+1}^m x_i x_j \zeta_{ij}. \quad (6)$$

The parameters ζ_{ij} and ξ_{ij} are used to define the shapes of the reducing temperature and density curves. These reducing parameters are not the same as the critical parameters of the mixture and are determined simultaneously in the nonlinear fit of experimental data with the other parameters of the mixture model.

Three excess functions were developed for the mixtures studied in this work. The excess function for the mixture Helmholtz energy for these three models is expressed as

$$\frac{a^E}{RT} = \alpha^E(\delta, \tau, \mathbf{x}) = \left\{ \sum_{i=1}^{m-1} \sum_{j=i+1}^m x_i x_j F_{ij} \right\} \sum_{k=1}^q N_k \delta^{d_k} \tau^{t_k} \exp(-\delta^{l_k}), \quad (7)$$

where the coefficients and exponents were obtained from nonlinear regression of experimental mixture data. Values of the coefficients and exponents for this equation are given in Table 2.

The generalized factors and mixture parameters, F_{ij} , ζ_{ij} and ξ_{ij} , are given in Table 3.

The functions used for calculating pressure, compressibility factor, internal energy, enthalpy, entropy, Gibbs energy, isochoric heat capacity, isobaric heat capacity, and the speed of sound from Eqs. (19) and (20) are given as Eqs. (8-15). The first derivative of pressure with respect to density at constant temperature $(\partial p/\partial \rho)_T$, second derivative of pressure with respect to density at constant temperature $(\partial^2 p/\partial \rho^2)_T$, and first derivative of pressure with respect to temperature at constant density $(\partial p/\partial T)_\rho$ are given in Eqs. (16-18).

$$Z = \frac{p}{\rho RT} = 1 + \delta \left(\frac{\partial \alpha^r}{\partial \delta} \right)_\tau \quad (8)$$

$$\frac{u}{RT} = \tau \left[\left(\frac{\partial \alpha^0}{\partial \tau} \right)_\delta + \left(\frac{\partial \alpha^r}{\partial \tau} \right)_\delta \right] \quad (9)$$

$$\frac{h}{RT} = \tau \left[\left(\frac{\partial \alpha^0}{\partial \tau} \right)_\delta + \left(\frac{\partial \alpha^r}{\partial \tau} \right)_\delta \right] + \delta \left(\frac{\partial \alpha^r}{\partial \delta} \right)_\tau + 1 \quad (10)$$

$$\frac{s}{R} = \tau \left[\left(\frac{\partial \alpha^0}{\partial \tau} \right)_\delta + \left(\frac{\partial \alpha^r}{\partial \tau} \right)_\delta \right] - \alpha^0 - \alpha^r \quad (11)$$

$$\frac{g}{RT} = 1 + \alpha^0 + \alpha^r + \delta \left(\frac{\partial \alpha^r}{\partial \delta} \right)_\tau \quad (12)$$

$$\frac{c_v}{R} = -\tau^2 \left[\left(\frac{\partial^2 \alpha^0}{\partial \tau^2} \right)_\delta + \left(\frac{\partial^2 \alpha^r}{\partial \tau^2} \right)_\delta \right] \quad (13)$$

$$\frac{c_p}{R} = \frac{c_v}{R} + \frac{\left[1 + \delta \left(\frac{\partial \alpha^r}{\partial \delta} \right)_\tau - \delta \tau \left(\frac{\partial^2 \alpha^r}{\partial \delta \partial \tau} \right) \right]^2}{\left[1 + 2\delta \left(\frac{\partial \alpha^r}{\partial \delta} \right)_\tau + \delta^2 \left(\frac{\partial^2 \alpha^r}{\partial \delta^2} \right)_\tau \right]} \quad (14)$$

$$\frac{w^2 M}{RT} = \frac{c_p}{c_v} \left[1 + 2\delta \left(\frac{\partial \alpha^r}{\partial \delta} \right)_\tau + \delta^2 \left(\frac{\partial^2 \alpha^r}{\partial \delta^2} \right)_\tau \right] \quad (15)$$

$$\left(\frac{\partial p}{\partial \rho} \right)_T = RT \left[1 + 2\delta \left(\frac{\partial \alpha^r}{\partial \delta} \right)_\tau + \delta^2 \left(\frac{\partial^2 \alpha^r}{\partial \delta^2} \right)_\tau \right] \quad (16)$$

$$\left(\frac{\partial^2 p}{\partial \rho^2} \right)_T = \frac{RT}{\rho} \left[2\delta \left(\frac{\partial \alpha^r}{\partial \delta} \right)_\tau + 4\delta^2 \left(\frac{\partial^2 \alpha^r}{\partial \delta^2} \right)_\tau + \delta^3 \left(\frac{\partial^3 \alpha^r}{\partial \delta^3} \right)_\tau \right] \quad (17)$$

$$\left(\frac{\partial p}{\partial T}\right)_p = R\rho \left[1 + \delta \left(\frac{\partial \alpha^r}{\partial \delta} \right)_\tau - \delta \tau \left(\frac{\partial^2 \alpha^r}{\partial \delta \partial \tau} \right) \right] \quad (18)$$

The ideal gas and residual Helmholtz energy for the mixtures required to calculate all single phase thermodynamic properties, given in Eqs. (8-18) above, are

$$\alpha^0 = \sum_{i=1}^m x_i \left[\frac{a_i^0(\rho, T)}{RT} + \ln x_i \right] \text{ and} \quad (19)$$

$$\alpha^r = \sum_{i=1}^m x_i \alpha_i^r(\delta, \tau) + \alpha^E(\delta, \tau, \mathbf{x}), \quad (20)$$

where α_i^r is the reduced residual Helmholtz energy of component i , a_i^r/RT .

If equations for the ideal gas Helmholtz energy in the nondimensional form $\alpha_i^0(\delta, \tau)$ are used rather than equations in the dimensional form $a_i^0(\rho, T)$ as indicated by Eq. (19), the following reducing variables

$$\delta = \rho / \rho_{c_i} \text{ and} \quad (21)$$

$$\tau = T_{c_i} / T, \quad (22)$$

must be used in the ideal gas equation rather than the reducing values defined by Eqs. (3) and (4). This does not apply to the residual part of the Helmholtz energy. The residual and excess terms $\alpha_i^r(\delta, \tau)$ and $\alpha^E(\delta, \tau, \mathbf{x})$ in Eq. (20) must be evaluated at the reduced state point of the mixture defined by Eqs. (3) and (4). This complication is avoided though the use of dimensional equations for functions involving the ideal gas heat capacity such as

$$a^0 = -RT + RT \ln \frac{\rho T}{\rho_0 T_0} + h_{0i}^0 - TS_{0i}^0 + \int_{T_0}^T c_{pi}^0 dT - T \int_{T_0}^T \frac{c_{pi}^0}{T} dT \quad (23)$$

Equations of the form

$$\alpha^0 = \ln \delta + N_0 \ln \tau + \sum_{i=1}^n N_i \tau^i + \dots \quad (24)$$

are derived from dimensional equations, and the critical parameters of the pure fluids are built into the coefficients of the equations. Additional information on the mixing function and its

derivatives, as well as formulas for other thermodynamic properties, can be found in Lemmon *et al.* (2000), which presents equations for mixtures of nitrogen, argon, and oxygen.

Vapor-Liquid Equilibrium (VLE) Properties

In a two-phase non-reacting mixture, the thermodynamic constraints for vapor-liquid equilibrium (VLE) are

$$T' = T'' = T, \quad (25)$$

$$p' = p'' = p, \text{ and} \quad (26)$$

$$\mu'_i = \mu''_i, \quad i=1, 2, \dots, m, \quad (27)$$

where the superscripts ' and " refer to the liquid and vapor phases, respectively, and m is the number of components in the mixture. Equation (27) is equivalent to equating the fugacities of the liquid and vapor phases for each component in the mixture,

$$f'_i = f''_i. \quad (28)$$

The chemical potential of component i in a mixture is

$$\mu_i(\rho, T) = \left(\frac{\partial A}{\partial n_i} \right)_{T, V, n_j} = \mu_i^c(T) + RT \ln(f_i), \quad (29)$$

where $\mu_i^c(T)$ is a function of temperature only and the notation n_j indicates that all mole numbers are held constant except n_i . The chemical potential in an ideal gas mixture is

$$\mu_i^0 = \left(\frac{\partial A^0}{\partial n_i} \right)_{T, V, n_j} = \mu_i^c(T) + RT \ln(f_i^0), \quad (30)$$

where f_i^0 is the ideal gas partial pressure of constituent i , $x_i p^0 = x_i \rho RT$. Subtracting equation (29) from equation (30) and solving for f_i results in

$$f_i = x_i \rho RT \exp \left(\frac{\partial (n \alpha^r)}{\partial n_i} \right)_{T, V, n_j}, \quad (31)$$

where α^r was defined in Eq. (20). The partial derivative at constant temperature, constant total volume (not molar volume), and constant mole numbers of all constituents except i is generally evaluated numerically.

Comparisons to Data

The accuracies of calculated values of various properties are determined by comparisons with measured values. Statistical analyses are used to determine the overall estimated accuracy of the model, and to define the ranges of estimated accuracies for various properties calculated with the formulation. Summary comparisons of values calculated using the mixture equation to p - ρ - T data, isochoric heat-capacity data (c_v), sound-speed data (w), and VLE data for refrigerant mixtures are given in Table 4, along with the temperature range of the data and the composition range for the first component listed. Compositions for VLE data are bubble-point compositions except for datasets where only the vapor phase compositions were reported.

In a few cases, individual data points were eliminated from the comparisons when the deviation for a particular point was much higher than those for other points by the same author in the same region. For density, individual data points were typically deleted when the deviation exceeded 10%. However, when the deviations slowly increased point by point, showing increasing differences in a particular region, these data points were left in the comparisons. This eliminates the likelihood of including in the comparisons data points which are in error and those which are reported incorrectly including obvious typographical errors in published manuscripts.

The statistics used to evaluate the equation are based on the percent deviation for any property, X ,

$$\% \Delta X = 100 \left(\frac{X_{\text{data}} - X_{\text{calc}}}{X_{\text{data}}} \right). \quad (32)$$

Using this definition, the average absolute deviation in Table 4 is defined as:

$$\text{AAD} = \frac{1}{n} \sum_{i=1}^n |\% \Delta X_i| \quad (33)$$

The comparisons given in the sections below for the various binary and ternary mixtures compare the equation of state to the experimental data using the average absolute deviation as given by Equation (33). Discussions of maximum errors or of systematic offsets always use the absolute values of the deviations.

The comparisons of the mixture model to experimental data exhibit many general trends as shown in the figures presented in this section. In these figures, data of a given type are separated into temperature increments of 10 K, where the temperatures listed at the top of each

small plot is the lower bound of this range. The details of the comparisons to $p\varphi T$ and VLE data are given below. Comparisons to $p\varphi T$ data, for the most part, focus on deviations in density, given inputs of pressure and temperature. However, in the critical region, deviations in density are generally higher than in the liquid or vapor phases, and several of the systems described below include comparisons based on deviations in pressure, given inputs of density and temperature. For the VLE data, the comparisons given in the following sections will focus on the percent difference in bubble point pressure. There are some VLE systems for which only the vapor phase compositions were reported, and the percent deviation in bubble point pressure is replaced with the percent deviation in dew point pressure in such cases.

The R-32/125 System

The R-32/125 system is perhaps the most widely studied system of all mixtures that have ever been measured. The data span the entire composition range and were measured at temperatures and pressures that cover nearly the entire range of practical fluid states. Further experimental data for the region at temperatures above 380 K would be of use for verifying the accuracy of the mixture model in this region.

Comparisons of experimental density data for the R-32/125 binary mixture to the mixture model are shown in Figure 1. For the datasets of Benmansour and Richon (1997, 1999), only one out of every 30 points are shown due to the very large number of data points published by these authors. All of the temperature, pressure, and composition ranges covered by Benmansour and Richon are shown in the figures, but the smaller set used for plotting allows the symbol shapes to be seen in the plots. In the liquid phase at temperatures below 360 K, the datasets of Kleemiss (1997), Magee and Haynes (2000), and Magee (2002) are represented on average to within 0.03%. The equation represents the data of Widiatmo *et al.* (1993), Piao *et al.* (1996), Perkins (2002) and Weber and Defibaugh (1994) with average deviations of 0.1%. Comparisons with the data of Benmansour and Richon (1997, 1999) show slightly higher deviations (about 0.17%). The data of Benmansour and Richon (1999) (in the liquid phase) agree favorably with the equation, except the data at 330 K, which have a systematic offset of about 0.3%, and do not agree with other data at this temperature. The AAD for this dataset in the liquid is 0.06% if the data at 330 K are omitted. The data of Piao *et al.* show systematic offsets near 263 and 273 K (disagreeing with other data in the same region and composition), but the average differences fall to 0.08% at higher temperatures.

The scatter between various experimental datasets is much higher in the vapor region than in the liquid. Several sets shows deviations between 0.02% and 0.18% on average from the equation, these being the data of Kleemiss (0.02%), Kiyoura *et al.* (1996), Sato *et al.* (1996), Weber and Defibaugh (1994), and Zhang *et al.* (1996). Differences are greater for other datasets.

Above 360 K, deviations in the area near the critical region and at even higher temperatures tend to increase, with the maximum errors in the datasets of Kiyoura *et al.* (1996) and Sato *et al.* (1996) reaching 0.3% in density. Comparisons with the data of Kleemiss show smaller differences, but even for this dataset, the model shows offsets of 0.15% at the highest temperatures. In the close vicinity of the critical point, it is not useful to compare deviations in density, even a slight change in pressure in this region can cause large changes in the density, with differences easily exceeding 5%; deviations in pressure are more meaningful. Above 340 K, the average absolute deviation in pressure is approximately 0.1% for all datasets. Even as the critical points of the mixtures at different compositions are approached (339-351 K, 3.6-5.8 MPa), the maximum deviations do not exceed approximately 0.3% in pressure. For the commercial mixture R-410A (the 50/50 by mass mixture of R-32 and R-125), there are four datasets within the region 4-10 mol/dm³: Kishizawa *et al.* (1999), Magee (2002), Perkins (2002), and Piao *et al.* (1996), with data points of Kishizawa *et al.* and Perkins near the critical point. The equation shows close agreement with the data of Perkins, with an average deviation of 0.16% in density (including the very near critical region) and 0.07% in pressure.

Comparisons to bubble point pressures are shown in Figure 2. Eliminating the data points that fall substantially outside the main body of VLE data in terms of their deviations from the mixture model, bubble point pressures are represented on average within 0.4%. The data of Kleemiss (1997), which are represented with an AAD of 0.05%, were the primary data used in the development of the model given here. However, nearly all of the other data points from various authors are represented within a band of $\pm 1\%$. Other datasets that are in good agreement with the data of Kleemiss include Defibaugh and Morrison (1995), 0.26%, Holcomb *et al.* (1998), 0.27%, Weber (2000), 0.32%, Oguchi *et al.* (1995), 0.36%, and Widiatmo *et al.* (1993), 0.4%. No systematic offsets are seen in the comparisons. In the few cases where both bubble and dew point compositions are given, differences between the calculated and experimental dew point compositions are generally within 0.005 mole fraction, where the dew point compositions

(and mixture pressure) were calculated given the mixture temperature and bubble point compositions.

The R-32/134a System

Comparisons of calculated mixture densities to experimental density data for the R-32/134a binary mixture are shown in Figure 3. The data of Kleemiss (1997) and of Magee and Haynes (2000) are represented on average to within 0.06%. Between 210 and 360 K, the average representation is 0.024%. The data of Magee between 200 and 210 K for the 0.33 mole fraction of R-32 show an offset of -0.3%; similar offsets were seen in other models, including that of Tillner-Roth *et al.* (1998) published by the JSRAE and in the earlier model of Lemmon and Jacobsen (1999). The vapor phase data of Kleemiss at 370 and 390 K cannot both be represented simultaneously within the stated experimental accuracy of the data. In this work, the equation is biased towards the data at 390 K, causing the higher deviations of calculated values at 370 K. Excluding the data at 273 and 283 K (which appear to be in error with deviations greater than 1%) at a composition of 0.45 mole fraction of R-32, values from the equation deviate from the data of Piao below 360 K on average by 0.21%. The data of Piao above 360 K show increasing scatter due to the complexity of modeling the critical region. Below 330 K in the vapor phase, the data of Oguchi *et al.* (1995) and Widiatmo *et al.* (1994, 1997) show average deviations of 0.1%. Above 330 K, in the area around the critical region, the scatter in the data and the deviations from the equation increase substantially. Deviations between the equation and the data of Oguchi *et al.* (1995, 1999), Sato *et al.* (1994), and Weber and Defibaugh (1994) are around 0.3%, with systematic differences of values from the equation with the data.

Comparisons to VLE data (see Figure 4) for the R-32/134a system show nearly the same trends as the R-32/125 system. In a similar fashion, eliminating the extraneous data points outside the main group of data, VLE data are generally represented with an AAD of 0.6%. All of the datasets appear to be of similar quality. Average differences are 0.38%, 0.41%, 0.50%, and 0.57% for the datasets of Takagi *et al.* (1999), Piao *et al.* (1996), Kim and Park (1999), and Chung and Kim (1997), respectively. For those datasets which reported both liquid and vapor composition, differences in the dew point composition are generally around 0.006 mole fraction.

The R-125/134a, R-125/143a, R-134a/143a, and R-134a/152a Systems

Comparisons of calculated densities to the experimental data for the R-125/134a binary mixture are shown in Figure 5. The data of Kleemiss (1997) and of Magee and Haynes (2000)

are represented on average to within 0.07%. Below 360 K, the average representation is 0.05%. In the liquid phase at 240 K, there is a systematic offset of 0.06% compared to the data of Kleemiss. This offset decreases quickly with increasing temperature. In the vapor phase, the average absolute deviation of the equation from the data of Widiatmo *et al.* (1997) is 0.09%. At the highest temperatures above the critical point, differences from the data of Kleemiss increase to a maximum of 0.26% at pressures around the critical pressure. Similar trends are found in the JSRAE model at the high temperatures, but with a maximum deviation of 0.20%.

Comparisons of experimental density data to the R-125/143a binary mixture are shown in Figure 6. Differences between the equation and the data of Kleemiss (1997) and of Magee and Haynes (2000) are around 0.06%. Below 360 K, differences fall (on average) to 0.03% for these two datasets. In the vapor phase, comparisons with the data of Widiatmo *et al.* (1994), Weber and Defibaugh (1994) and Zhang *et al.* (1998) show differences of 0.17%.

Comparisons for the R-134a/143a system are shown in Figure 7. Below 360 K, comparisons with the equation show differences (on average) of 0.03% in the liquid and vapor phases. In the vapor phase, comparisons with the data of Widiatmo *et al.* (1994), Weber and Defibaugh (1994) and Zhang *et al.* (1998) show differences of 0.17%. Above 360 K, the differences increase at pressures near the critical pressure of the mixture, but decrease to low levels at lower and higher pressures. Similar comments can be made about the R-134a/152a system (see Figure 8); differences below 360 K, as well as at conditions above 360 K away from the critical pressure of the mixture are about 0.06%. As the critical region is approached, differences increase up to 0.5%. Although there are few publications of measurements for this system, it was covered in detail by Tillner-Roth (1993) for a wide range of temperature and pressure, for several compositions (0.25, 0.50, and 0.75 mole fraction). These data are well represented by the model reported here.

The comparisons to VLE data for the R-125/134a, R-125/143a, and R-134a/143a binary mixtures (see Figure 9) are very similar to those described above for the R-32/125 and R-32/134a systems. The average absolute deviation for each system is approximately 0.5% in bubble point pressure. Comparisons with the dew point compositions are similar to those for the other systems previously described. The R-134a/152a system shows similar trends above 270 K, but at lower temperatures, there appears to be a systematic offset of calculated bubble point pressures

compared to the data of Defibaugh and Morrison (1995) and Kleiber (1994), with a maximum difference of 2.4% in pressure for both of these datasets.

The Ternary Mixtures

The R-32/125/134a system is unique from a modeling standpoint since it combines the three mixture equations (the individual equations for R-32/125 and R-32/134a, and the generalized equation for R-125/134a). No additional parameters were required to model the ternary mixture, although slight systematic offsets are seen in several locations. Comparisons of the combined mixture model for this ternary mixture are shown in Figure 10. In the liquid region below 360 K, the equations represent the data of Magee (2000), Kleemiss (1997), and Benmansour and Richon (1999) with an average deviation of 0.06%. At temperatures near 260 K, systematic offsets of 0.04% and 0.08% are seen for the datasets of Kleemiss and Magee, respectively. In the vapor region (below 360 K), differences are about 0.06% for the data of Kleemiss, but increase to 0.5% for the data of Benmansour and Richon and of Piao *et al.* (1996). Above 360 K, differences continue to increase, with maximum deviations of 0.5% for the data of Kleemiss and higher for other datasets. The scatter among various authors is greater than 0.5% in density near the critical region as expected.

Figure 11 illustrates comparisons of VLE data for the R-32/125/134a ternary mixtures. Bubble point pressures are represented on average to within 0.7% and dew point composition differences are within 0.005 mole fraction of R-32. Comparisons to the data of Nagel and Bier (1995) show deviations of 0.26% and those with Piao *et al.* (1996) show deviations of 0.66%.

Although the ternary mixture R-125/134a/143a has no additional fitted parameters, the properties of this system are represented with accuracies similar to those of the binary mixtures. The experimental data of Kleemiss (1997) are represented on average by differences of 0.03%. Small systematic differences are evident in the comparisons given in Figure 12, such as the offset of 0.05% at 300 K. Trends above 360 K in the critical region are similar to those described for the binary mixtures above. Figure 11 also includes comparisons of VLE data for the R-125/134a/143a ternary mixture. There are very few saturation data for this mixture, but the data of Nagel and Bier (1995) and those of Kleemiss (1997) are in agreement within about 1% in bubble point pressure, with an AAD of 0.35%.

Other thermodynamic properties

The isochoric heat capacity has been measured by Magee (2002) for four of the binary mixtures: R-32/125, R-32/134a, R-125/134a, and R-125/143a. Figure 13 shows comparisons of values calculated from the model to these data. In addition, comparisons to the experimental data for the R-32/125/134a ternary mixture are shown in Figure 14. In general, the mixture model represents the data with an average absolute deviation between 0.3 and 0.5% for the binary mixtures, and 0.3% for the ternary mixture. There is very little systematic behavior in the deviations for the systems studied, and the model represents the data to within their experimental uncertainty.

Comparisons to the saturated liquid isobaric heat capacity data of Gunther and Steimle (1996) for the seven mixtures which they studied show very comparable deviations, with differences generally less than 1% for most of the mixtures except near the lowest temperatures (200 K) and near the critical region (where c_p tends to increase rapidly with increasing temperature). The R-134a/152a system is the only exception, with deviations of less than 1% at the highest temperatures, but with steadily increasing deviations at lower temperatures, with a maximum of 5% at 200 K. This is the only system with vapor measurements, and the model represents these data (Türk *et al.*, 1996) with an average absolute deviation of 0.37%.

Speed of sound measurements in the vapor phase for the R-32/125, R-32/134a, R-125/134a, R-125/143a, and R-32/125/134a mixtures were given by Hozumi (1996), Hurley *et al.* (1997), and Ichikawa *et al.* (1998). Comparisons of the model to these data are shown in Figure 15 for the binary mixtures and Figure 16 for the ternary mixture. The average absolute deviations for these systems range between 0.01 and 0.04% in the speed of sound. In the liquid phase of the R-134a/152a system, the mixture model represents the speed of sound measurements of Beliajeva *et al.* (1999) and Grebenkov *et al.* (1994) within an average absolute deviation of about 0.3% as shown in Figure 17.

Accuracy Assessment

Based on comparisons to experimental data, the equation is generally accurate to 0.1% in density, 0.5% in heat capacity and speed of sound, and 0.5% for calculated bubble point pressures. The model is valid from 200 to 450 K up to 60 MPa as verified by experimental data. Although the equation was developed using mostly binary data, it is accurate in calculating the

properties of the two ternary mixtures for which data were available for comparison. It is expected that this result will apply to other ternary and higher-order systems as well. Future measurements are needed to confirm whether the equation is valid for other mixtures and in regions not covered by the experimental data used in the development of this model. Such data will enable continued evaluation and refinement of the model and modeling process. While early measurements of mixture properties were considered to be less accurate than those for pure substances, modern mixture data are approaching the accuracy of the best pure substance measurements. Refinements in the equations of state for both pure substances and mixtures will improve the prediction of properties for fluid mixtures as they become more common as working fluids in engineered systems.

Acknowledgments

This work was funded by the 21-CR research program of the Air-Conditioning and Refrigeration Technology Institute; the Office of Building Technology, State and Community Programs of the U.S. Department of Energy; and by NIST. We thank Dr. Mark McLinden of NIST, Boulder, for his assistance and suggestions during the development and documentation of the equation.

References

Beliajeva, O. V., A. J. Grebenkov, T. A. Zajatz, and B. D. Timofejev, Int. J. Thermophys. 20, 1689 (1999).

Benmansour, S. and D. Richon, The International Electronic Journal of Physico-Chemical Data 3, 149 (1997).

Benmansour, S. and D. Richon, The International Electronic Journal of Physico-Chemical Data 4, 29 (1998).

Benmansour, S. and D. Richon, The International Electronic Journal of Physico-Chemical Data 5, 127 (1999).

Benmansour, S. and D. Richon, The International Electronic Journal of Physico-Chemical Data 5, 9 (1999).

Bouchot, C. and D. Richon, The International Electronic Journal of Physico-Chemical Data 4, 163 (1998).

Chung, E. Y. and M. S. Kim, J. Chem. Eng. Data 42, 1126 (1997).

Defibaugh, D. R. and G. Morrison, Int. J. Refrig. 18, 518 (1995).

Dressner, M. and K. Bier, Fortschr.-Ber. VDI 3 (1993).

Fujiwara, K., H. Momota, and M. Noguchi, 13th Japan Symp. Thermophys. Prop. A11.6, 61 (1992).

Fujiwara, K., S. Nakamura, and M. Noguchi, *J. Chem. Eng. Data* 43, 967 (1998).

Grebennov, A. J., Yu. G. Kotelevsky, V. V. Saplitza, O. V. Beljaeva, T. A. Zajatz, and B. D. Timofeev, *Proc, CFC's: The Day After, IIR Comm* B1, B2, E1, E2, p. 21 (1994).

Gunther, D. and F. Steimle, *Int. J. Refrig.* 20, 235 (1996).

Higashi, Y., *Int. J. Thermophys.* 16, 1175 (1995).

Higashi, Y., *J. Chem. Eng. Data* 42, 1269 (1997).

Higashi, Y., *J. Chem. Eng. Data* 44, 328 (1999).

Higashi, Y., *J. Chem. Eng. Data* 44, 333 (1999).

Higashi, Y., private communication, Iwaki Meisei University, Japan (1996).

Higuchi, M. and Y. Higashi, *Proc. 16th Japan Symp. Thermophys. Prop.*, Hiroshima, p. 5 (1995).

Holcomb, C. D., J. W. Magee, J. Scott, S. L. Outcalt, and W. M. Haynes, *Selected Thermodynamic Properties for Mixtures of R-32 (difluoromethane), R-125 (pentafluoroethane), R-134A (1,1,1,2-tetrafluoroethane), R-143A (1,1,1-trifluoroethane), R-41 (fluoromethane), R-290 (propane), and R-744 (carbon dioxide)*, National Institute of Standards and Technology, Tech Note 1397 (1998).

Hozumi, T., H. Sato, and K. Watanabe, *4th Asian Thermophysical Properties Conference, Japan*, p. 307 (1995).

Hozumi, T., private communication, Keio University, Yokohama, Japan (1996).

Hurly, J. J., J. W. Schmidt, and K. A. Gillis, *Int. J. Thermophys.* 18, 655 (1997).

Ichikawa, T., K. Ogawa, H. Sato, and K. Watanabe, *Speed-of-Sound Measurements for Gaseous Pentafluoroethane and Binary Mixture of Pentafluoroethane + 1,1,1-Trifluoroethane*, Department of System Design Engineering, Faculty of Science and Technology, Keio University, Yokohama, Japan (1998).

Kato, R., K. Shirakawa, and H. Nishiumi, *Fluid Phase Equilib.* 194, 995 (2002).

Kim, C.-N. and Y.-M. Park, *Int. J. Thermophys.* 20, 519 (1999).

Kim, C.-N., E.-H. Lee, Y.-M. Park, J. Yoo, K.-H. Kim, J.-S. Lim, and B.-G. Lee, *Int. J. Thermophys.* 21, 871 (2000).

Kiyoura, H., J. Takebe, H. Uchida, H. Sato, and K. Watanabe, *J. Chem. Eng. Data* 41, 1409 (1996).

Kleemiss, M., *Fortschr.-Ber. VDI* 19 (1997).

Kleiber, M., *Fluid Phase Equilib.* 92, 149 (1994).

Kubota, H. and T. Matsumoto, *J. Chem. Eng. Japan* 26, 320 (1993).

Lemmon, E. W. and R. T Jacobsen, *in preparation* (2002).

Lemmon, E. W. and R. T Jacobsen, *Int. J. Thermophys.* 20, 825 (1999).

Lemmon, E. W. and R. T Jacobsen, *J. Phys. Chem. Ref. Data* 29, 521 (2000).

Lemmon, E. W. and R. Tillner-Roth, *Fluid Phase Equilibria* 165, 1 (1999).

Lemmon, E. W., *A Generalized Model for the Prediction of the Thermodynamic Properties of Mixtures Including Vapor-Liquid Equilibrium*, Ph.D. Dissertation, University of Idaho, Moscow (1996).

Lemmon, E. W., R. T Jacobsen, S. G. Penoncello, and D. G. Friend, *J. Phys. Chem. Ref. Data* 29, 331 (2000).

Lim, J. S., J.-Y. Park, B.-G. Lee, and Y.-W. Lee, *Fluid Phase Equilib.* 193, 29 (2002).

Magee, J. W. and W. W. Haynes, *Int. J. Thermophys.* 21, 113 (2000).

Magee, J. W., *Int. J. Thermophys.* 21, 151 (2000).

Magee, J. W., *Int. J. Thermophys.* 21, 95 (2000).

Magee, J. W., private communication, NIST, Boulder, Colorado (2002).

Nagel, M. and K. Bier, *Int. J. Refrig.* 18, 534 (1995).

Nagel, M. and K. Bier, *Int. J. Refrig.* 19, 264 (1996).

Oguchi, K., K. Amano, T. Namiki, and N. Umezawa, *Int. J. Thermophys.* 20, 1667 (1999).

Oguchi, K., T. Takaishi, N. Yada, T. Namiki, and T. Sato, private communication, Kanagawa Institute of Technology, Japan (1995).

Outcalt, S. L. and M. O. McLinden, *J. Phys. Chem. Ref. Data* 25, 605 (1996).

Perkins, R. A., private communication, NIST, Boulder, Colorado (2002).

Piao, C.-C., I. Iwata, and M. Noguchi, private communication, Mech. Eng. Lab., Daikin Industries, Ltd., Japan (1996).

Sand, J. R., S. K. Fischer, and J. A. Jones, *Int. J. Refrig.* 17, 123 (1994).

Sato, T., H. Kiyoura, H. Sato, and K. Watanabe, *Int. J. Thermophys.* 17, 43 (1996).

Sato, T., H. Kiyoura, H. Sato, and K. Watanabe, *J. Chem. Eng. Data* 39, 855 (1994).

Schramm, B., J. Hauck, and L. Kern, *Ber. Bunsenges. Phys. Chem.* 96, 745 (1992).

Shimawaki, S., K. Fujii, and Y. Higashi, *Int. J. Thermophys.* 23, 801 (2002).

Tack, A. and K. Bier, *Fortschr.-Ber. VDI* 3, 1 (1997).

Takagi, T., T. Sakura, T. Tsuji, and M. Hongo, *Fluid Phase Equilib.* 162, 171 (1999).

Tillner-Roth, R. and A. Yokozeki, *J. Phys. Chem. Ref. Data* 25, 1273 (1997).

Tillner-Roth, R. and H. D. Baehr, *J. Phys. Chem. Ref. Data* 23, 657 (1994).

Tillner-Roth, R., *J. Chem. Thermodyn.* 25, 1419 (1993).

Tillner-Roth, R., J. Li, A. Yokozeki, H. Sato, and K. Watanabe, *Thermodynamic Properties of Pure and Blended Hydrofluorocarbon (HFC) Refrigerants*, Japan Society of Refrigerating and Air Conditioning Engineers, Tokyo (1998).

Tuerk, M., M. Crone, and K. Bier, *J. Chem. Thermodyn.* 28, 1179 (1996).

Uchida, H., H. Sato, and K. Watanabe, *Int. J. Thermophys.* 20, 97 (1999).

Weber, F., *Fluid Phase Equilib.* 174, 165 (2000).

Weber, L. A. and D. R. Defibaugh, *Int. J. Thermophys.* 15, 863 (1994).

Widiatmo, J. V., H. Sato, and K. Watanabe, *Fluid Phase Equilib.* 99, 199 (1994).

Widiatmo, J. V., H. Sato, and K. Watanabe, *High Temp.-High Press.* 25, 677 (1993).

Widiatmo, J. V., H. Sato, and K. Watanabe, *Int. J. Thermophys.* 16, 801 (1994).

Widiatmo, J. V., T. Fujimine, H. Sato, and K. Watanabe, *J. Chem. Eng. Data* 42, 270 (1997).

Yokoyama, C., T. Nishino, and M. Takahashi, *Fluid Phase Equilib.* 174, 231 (2000).

Zhang, H.-L., H. Sato, and K. Watanabe, *J. Chem. Eng. Data* 41, 1401 (1996).

Zhang, H.-L., S. Tada, H. Sato, and K. Watanabe, *Fluid Phase Equilib.* 151, 333 (1998).

Table 1. Pure fluid equations of state for the refrigerants used in the mixture model

Fluid	Author	Temperature Range (K)	Maximum Pressure (MPa)
R-32	Tillner-Roth and Yokozeki (1997)	136.34 – 435	70
R-125	Lemmon and Jacobsen (2002)	172.52 – 500	60
R-134a	Tillner-Roth and Baehr (1994)	169.85 – 455	70
R-143a	Lemmon and Jacobsen (2000)	161.34 – 650	100
R-152a	Outcalt and McLinden (1996)	154.56 – 500	60

Table 2. Coefficients and exponents of the mixture equations

k	N_k	t_k	d_k	l_k
R-32/125				
1	-0.0060247	4.8	2	1
2	0.071296	0.52	5	1
3	0.59146	1.9	1	2
4	0.59569	1.05	3	2
5	0.014007	0.54	9	2
6	-0.35902	2.7	2	3
7	0.11189	9.0	3	3
8	-0.066286	3.7	6	3
R-32/134a				
1	0.22909	1.9	1	1
2	0.094074	0.25	3	1
3	0.00039876	0.07	8	1
4	0.021133	2.0	1	2
R-125/134a, R-125/143a, R-134a/143a, R-143a/152a				
1	-0.013073	7.4	1	1
2	0.018259	0.35	3	1
3	0.0000081299	10.0	11	2
4	0.0078496	5.3	2	3

Table 3. Parameters of the mixture equations

Binary Mixture	ζ_{ij} (K)	ξ_{ij} (dm ³ · mol ⁻¹)	F_{ij}
R-32/125	24.85	-0.005212	1.0
R-32/134a	7.909	-0.002039	1.0
R-125/134a	-0.4326	-0.0003453	1.0
R-125/143a	5.551	-0.0004452	1.1697
R-134a/143a	2.324	0.0006182	0.5557
R-134a/152a	4.202	0.004223	2.0

Table 4. Summary comparisons of mixture properties calculated from the model to refrigerant mixture data

Author	No. Points	Pressure Range (MPa)	Density Range (mol/dm ³)	Temperature Range (K)	Composition Range (mole fraction)	AAD ^a (%)
R-32/125 — $p\varphi T$						
Benmansour and Richon (1997)	12909	0.14-19	0.0661-17.8	253-333	0.697	0.265
Benmansour and Richon (1999)	26777	0.107-19.9	0.0494-18.2	252-332	0.0931-0.884	0.627
Holcomb <i>et al.</i> (1998)	45	0.896-4.6	0.719-19.2	279-341	0.236-0.955	0.908
Kiyoura <i>et al.</i> (1996)	94	1.82-5.24	0.829-1.72	330-440	0.367-0.605	0.134
Kleemiss (1997)	415	0.0185-17.1	0.0073-16.2	243-413	0.503-0.508	0.0459
Magee (2002)	235	4.07-35.3	8.57-19.6	200-400	0.697	0.047
Magee and Haynes (2000)	228	2.57-35.3	1.06-17.3	200-400	0.499	0.04
Oguchi <i>et al.</i> (1995)	6	6.3-16.8	8.34-8.37	355-430	0.874	0.129
Perkins (2002)	411	3.85-19	6.54-14.7	300-398	0.697	0.116
Piao <i>et al.</i> (1996)	543	0.54-15	0.286-17.3	263-393	0.365-0.902	0.277
Sato <i>et al.</i> (1996)	156	1.78-5.26	0.836-1.72	320-440	0.697-0.902	0.14
Weber (2000)	90	1.45-3.97	0.776-16.9	294-333	0.416-0.884	0.627
Weber and Defibaugh (1994)	17	0.304-4.22	0.105-1.9	338-373	0.545	0.185
Widiatmo <i>et al.</i> (1993)	24	0.884-2.3	10.2-18.2	279-309	0.204-0.902	0.0909
Zhang <i>et al.</i> (1996)	124	0.094-4.6	0.0298-2.01	300-380	0.500-0.697	0.0739
R-32/125 — VLE						
Benmansour and Richon (1999)	33	0.357-3.9		252-332	0.0931-0.884	0.511
Defibaugh and Morrison (1995)	10	0.348-4.3		249-338	0.763	0.339
Fujiwara <i>et al.</i> (1992)	8	0.69-0.817		273-273	0.055-0.895	2.03
Higashi (1997)	22	0.905-2.47		283-313	0.225-0.896	0.472
Holcomb <i>et al.</i> (1998)	30	0.829-4.58		279-340	0.339-0.947	0.252
Kato <i>et al.</i> (2002)	39	2.35-5.26		318-349	0.110-0.952	1.84
Kleemiss (1997)	23	0.108-3.68		223-333	0.482-0.517	0.0299
Nagel and Bier (1995)	34	0.0382-5.04		204-345	0.241-0.951	0.414
Oguchi <i>et al.</i> (1995)	11	0.361-5.65		249-350	0.874	0.287
Piao <i>et al.</i> (1996)	10	0.54-1.07		263-282	0.365-0.902	0.7
Takagi <i>et al.</i> (1999)	47	0.283-3.93		248-333	0.269-0.940	0.998
Weber (2000)	90	1.45-3.97		294-333	0.416-0.884	0.271
Widiatmo <i>et al.</i> (1993)	24	0.884-2.3		279-309	0.204-0.902	0.338
R-32/125 — Second Virial Coefficient						
Kiyoura <i>et al.</i> (1996)	23			330-440	0.394-0.632	2.2
Sato <i>et al.</i> (1996)	39			320-440	0.0978-0.302	1.94
Weber and Defibaugh (1994)	3			338-373	0.454	3.15
R-32/125 — Isochoric Heat Capacity						
Magee (2000)	111		11.4-17.1	207-344	0.499	0.448
Perkins (2002)	363	4.13-18.3		300-397	0.697	1.73
R-32/125 — Isobaric Heat Capacity						
Gunther and Steimle (1996)	89			203-313	0.434-0.874	0.854
R-32/125 — Sound Speed						
Hozumi <i>et al.</i> (1995)	178	0.0394-0.553		303-343	0.200-0.776	0.0439

Table 4. Summary comparisons of mixture properties calculated from the model to refrigerant mixture data (continued)

Author	No. Points	Pressure Range (MPa)	Density Range (mol/dm ³)	Temperature Range (K)	Composition Range (mole fraction)	AAD ^a (%)
R-32/134a — $p\varphi T$						
Holcomb <i>et al.</i> (1998)	44	0.523-4.28	0.805-17.2	279-340	0.130-0.972	1.13
Kleemiss (1997)	390	0.0187-17.1	0.0077-17.2	243-413	0.497-0.555	0.049
Magee and Haynes (2000)	461	2.7-35.4	1.1-18.4	200-400	0.328-0.499	0.0749
Oguchi <i>et al.</i> (1999)	61	0.285-16.6	0.115-12.9	310-473	0.391-0.886	0.355
Oguchi <i>et al.</i> (1995)	53	0.134-15.3	2-18.7	237-473	0.273-0.709	0.236
Piao <i>et al.</i> (1996)	643	0.241-15	0.121-16.2	260-393	0.328-0.886	0.376
Sato <i>et al.</i> (1994)	220	1.96-6.18	1-2.12	320-440	0.329-0.886	0.207
Weber and Defibaugh (1994)	17	0.33-4.29	0.121-2.17	338-373	0.508	0.905
Widiatmo <i>et al.</i> (1994)	30	0.576-3.09	10.9-18.5	279-339	0.329-0.886	0.172
Widiatmo <i>et al.</i> (1997)	22	1-3	11.9-14.6	279-329	0.395	0.11
R-32/134a — VLE						
Chung and Kim (1997)	34	0.199-3.13		263-323	0.207-0.759	0.571
Defibaugh and Morrison (1995)	25	0.263-4.46		252-358	0.495-0.550	0.515
Fujiwara <i>et al.</i> (1992)	6	0.384-0.758		273-273	0.203-0.922	3.14
Higashi (1995)	12	0.567-1.9		283-313	0.121-0.673	3.86
Holcomb <i>et al.</i> (1998)	48	0.379-4.56		279-340	0.162-0.783	0.427
Kim and Park (1999)	25	0.201-0.96		258-283	0.201-0.798	0.5
Kleemiss (1997)	16	0.0729-3.14		223-343	0.419-0.517	0.344
Nagel and Bier (1995)	50	0.0148-5.41		202-368	0.212-0.771	0.447
Oguchi <i>et al.</i> (1999)	36	0.173-5.01		243-361	0.391-0.886	2.44
Oguchi <i>et al.</i> (1995)	34	0.134-1.29		237-300	0.273-0.709	1.04
Piao <i>et al.</i> (1996)	10	0.241-0.93		260-283	0.328-0.886	0.411
Shimawaki <i>et al.</i> (2002)	40	0.251-1.39		263-293	0.135-0.923	0.492
Takagi <i>et al.</i> (1999)	35	0.084-3.34		243-333	0.183-0.807	2.58
Widiatmo <i>et al.</i> (1994)	30	0.576-3.09		279-339	0.329-0.886	1.69
R-32/134a — Second Virial Coefficient						
Sato <i>et al.</i> (1994)	57			320-440	0.113-0.671	2.91
Tack and Bier (1997)	10			333-398	0.500-0.518	3.47
Weber and Defibaugh (1994)	3			338-373	0.491	7.74
R-32/134a — Isochoric Heat Capacity						
Magee (2000)	131		13.2-18.3	205-342	0.499	0.31
R-32/134a — Isobaric Heat Capacity						
Gunther and Steinle (1996)	96			203-323	0.397-0.881	1.43
R-32/134a — Sound Speed						
Hozumi <i>et al.</i> (1995)	193	0.0308-0.241		303-343	0.155-0.895	0.016

Table 4. Summary comparisons of mixture properties calculated from the model to refrigerant mixture data (continued)

Author	No. Points	Pressure Range (MPa)	Density Range (mol/dm ³)	Temperature Range (K)	Composition Range (mole fraction)	AAD ^a (%)
R-125/134a — $p\varphi T$						
Holcomb <i>et al.</i> (1998)	17	0.537-2.54	0.528-11.8	280-342	0.349-0.719	0.236
Kleemiss (1997)	407	0.0186-17.1	0.00804-13.2	243-413	0.500-0.509	0.0459
Magee and Haynes (2000)	268	2.84-35.4	1.66-14.1	199-400	0.500	0.102
Weber and Defibaugh (1994)	18	0.169-4.03	0.0691-2.21	303-373	0.494	0.266
Widiatmo <i>et al.</i> (1997)	149	1-3.01	7.99-12.4	279-349	0.0865-0.923	0.0859
Yokoyama <i>et al.</i> (2000)	341	0.1-6.62	0.0289-4.48	298-423	0.250-0.751	0.816
R-125/134a — VLE						
Higashi (1999)	15	0.516-1.73		283-313	0.179-0.776	1.1
Higuchi and Higashi (1995)	25	0.412-2		283-313	0.179-0.776	0.847
Holcomb <i>et al.</i> (1998)	40	0.379-3.62		279-340	0.259-0.649	3.04
Kim and Park (1999)	35	0.201-1.57		263-303	0.0001-0.813	3.39
Kleemiss (1997)	24	0.0663-2.89		224-343	0.461-0.514	0.301
Nagel and Bier (1995)	31	0.0172-3.97		206-364	0.254-0.749	9.92
Widiatmo <i>et al.</i> (1997)	36	0.424-2.97		279-349	0.0865-0.923	1.28
R-125/134a — Second Virial Coefficient						
Weber and Defibaugh (1994)	4			323-373	0.505	2.52
R-125/134a — Isochoric Heat Capacity						
Magee (2000)	94		10-14	206-344	0.500	0.375
R-125/134a — Isobaric Heat Capacity						
Gunther and Steimle (1996)	73			203-323	0.222-0.718	0.877
R-125/134a — Sound Speed						
Hozumi (1996)	81	0.0405-0.528		303-343	0.348-0.693	0.02

Table 4. Summary comparisons of mixture properties calculated from the model to refrigerant mixture data (continued)

Author	No. Points	Pressure Range (MPa)	Density Range (mol/dm ³)	Temperature Range (K)	Composition Range (mole fraction)	AAD ^a (%)
R-125/143a — $p\varphi T$						
Holcomb <i>et al.</i> (1998)	14	0.798-2.56	0.611-11.4	279-328	0.349-0.672	0.996
Kleemiss (1997)	151	1.59-17.1	6.41-13.1	243-373	0.503	0.0369
Magee and Haynes (2000)	281	2.13-35.4	0.881-14	200-400	0.500	0.0749
Uchida <i>et al.</i> (1999)	7	0.—2	0.931-3.03	308-340	0.411	0.95
Weber and Defibaugh (1994)	27	0.217-3.27	0.0804-1.44	333-373	0.509	0.329
Widiatmo <i>et al.</i> (1994)	37	0.0999-0.199	8.16-11.7	279-329	0.0725-0.863	0.244
Zhang <i>et al.</i> (1998)	205	0.115-4.76	0.0366-2.53	305-390	0.273-0.736	0.136
R-125/143a — VLE						
Uchida <i>et al.</i> (1999)	7	1.64-3.46		308-340	0.411	0.3
Higashi (1999)	18	0.622-2		273-313	0.150-0.758	1.6
Holcomb <i>et al.</i> (1998)	36	0.767-2.63		279-326	0.286-0.650	0.832
Kleemiss (1997)	16	0.086-3.29		223-338	0.460-0.498	0.305
Nagel and Bier (1995)	19	0.0323-3.69		205-343	0.493-0.503	0.136
Widiatmo <i>et al.</i> (1994)	34	0.773-2.82		279-329	0.0725-0.863	0.723
R-125/143a — Second Virial Coefficient						
Tack and Bier (1997)	6			333-398	0.484-0.507	7.41
Uchida <i>et al.</i> (1999)	8			330-400	0.588	4.65
Weber and Defibaugh (1994)	5			333-373	0.490	5.28
R-125/143a — Isochoric Heat Capacity						
Magee (1996)	109		9.89-13.9	205-343	0.500	0.55
R-125/143a — Isobaric Heat Capacity						
Gunther and Steimle (1996)	73			203-318	0.192-0.671	0.831
R-125/143a — Sound Speed						
Ichikawa <i>et al.</i> (1998)	142	0.0404-0.548		303-343	0.199-0.803	0.0109
R-134a/143a — $p\varphi T$						
Holcomb <i>et al.</i> (1998)	17	0.522-2.81	0.661-12.2	280-343	0.281-0.650	1.33
Kleemiss (1997)	377	0.0921-17.1	0.0316-13.9	243-413	0.491-0.501	0.0529
R-134a/143a — VLE						
Higashi (1996)	10	0.521-2.81		280-340	0.349-0.650	0.819
Holcomb <i>et al.</i> (1998)	40	0.379-3.31		280-340	0.349-0.834	0.54
Kim <i>et al.</i> (2000)	54	0.2-1.83		263-313	0.0786-0.919	0.417
Kleemiss (1997)	18	0.0594-3.39		223-353	0.501-0.522	0.143
Kubota and Matsumoto (1993)	41	0.349-2.87		278-333	0.144-0.891	0.95
Lim <i>et al.</i> (2002)	35	0.293-1.82		273-313	0.081-0.905	0.756
Nagel and Bier (1995)	12	0.0214-3.93		205-360	0.503-0.526	0.68

Table 4. Summary comparisons of mixture properties calculated from the model to refrigerant mixture data (continued)

Author	No. Points	Pressure Range (MPa)	Density Range (mol/dm ³)	Temperature Range (K)	Composition Range (mole fraction)	AAD ^a (%)
R-134a/152a — <i>pρT</i>						
Dressner and Bier (1993)	139	0.281-56	0.0829-12.1	333-423	0.484-0.538	0.196
Tillner-Roth (1993)	1721	0.0885-16.9	0.0275-15.3	243-433	0.247-0.751	0.0509
Weber and Defibaugh (1994)	11	0.267-3.16	0.0939-1.68	353-373	0.496	0.16
R-134a/152a — VLE						
Defibaugh and Morrison (1995)	13	0.104-3.43		248-367	0.776	0.718
Kleiber (1994)	25	0.13-0.662		254-298	0.314-0.977	0.825
Sand <i>et al.</i> (1994)	4	0.27-0.285		273-273	0.117-0.758	2.43
Tillner-Roth (1993)	23	0.925-4.08		313-378	0.229-0.750	0.258
R-134a/152a — Second Virial Coefficient						
Schramm <i>et al.</i> (1992)	7			233-473		11.1
Weber and Defibaugh (1994)	2			353-373	0.503	5.4
R-134a/152a — Isobaric Heat Capacity						
Gunther and Steimle (1996)	32			203-323	0.137-0.720	2.63
Tuerk <i>et al.</i> (1996)	49	0.1-2.5		298-423	0.500	0.369
R-134a/152a — Sound Speed						
Beliajeva <i>et al.</i> (1999)	329	0.456-16.5		230-350	0.128-0.687	0.265
Grebennikov <i>et al.</i> (1994)	120	0.569-19		230-336	0.687	0.557

Table 4. Summary comparisons of mixture properties calculated from the model to refrigerant mixture data (continued)

Author	No. Points	Pressure Range (MPa)	Density Range (mol/dm ³)	Temperature Range (K)	Composition Range (mole fraction)	AAD ^a (%)
R-32/125/134a — $p\rho T$						
Benmansour and Richon (1998)	289	0.267-3.82	11-15.2	253-333	0.381	0.231
Benmansour and Richon (1999)	11623	0.119-15.2	0.0575-15.5	253-333	0.377	0.162
Holcomb <i>et al.</i> (1998)	42	0.229-3.93	0.711-15.3	243-345	0.200-0.676	0.975
Hurly <i>et al.</i> (1997)	88	0.321-7.78	0.0861-2.76	313-453	0.346	0.212
Kiyoura <i>et al.</i> (1996)	105	1.57-5.74	0.766-2.07	315-440	0.381-0.515	0.586
Kleemiss (1997)	369	0.0258-17.1	0.00857-15.4	243-413	0.334-0.348	0.083
Magee (2000)	352	2.97-35.1	1.57-17	199-400	0.333-0.380	0.118
Oguchi <i>et al.</i> (1995)	12	5.18-12.3	5.85-6.21	365-430	0.379-0.471	0.202
Piao <i>et al.</i> (1996)	1025	0.447-15	0.208-15.1	263-393	0.186-0.473	0.281
Widiatmo <i>et al.</i> (1997)	76	0.723-3.24	10.4-14.9	279-339	0.346-0.463	0.196
R-32/125/134a — VLE						
Benmansour and Richon (1999)	18	0.211-2.72		253-333	0.377	2.14
Higashi (1996)	36	0.556-2.73		273-323	0.173-0.540	1.01
Holcomb <i>et al.</i> (1998)	58	0.0729-3.93		220-345	0.0449-0.599	0.919
Kleemiss (1997)	44	0.0743-4.19		221-353	0.144-0.661	0.347
Nagel and Bier (1995)	29	0.0259-4.76		205-361	0.187-0.433	0.253
Piao <i>et al.</i> (1996)	31	0.447-2.41		269-326	0.317-0.381	0.65
Widiatmo <i>et al.</i> (1997)	20	0.723-3.24		279-339	0.346-0.463	0.93
R-32/125/134a — Second Virial Coefficient						
Hozumi <i>et al.</i> (1995)	11			340-440	0.250	8.47
Kiyoura <i>et al.</i> (1996)	11			340-440	0.179	2.75
R-32/125/134a — Isochoric Heat Capacity						
Magee (2000)	147		11.4-17	202-344	0.333-0.380	0.28
R-32/125/134a — Isobaric Heat Capacity						
Gunther and Steimle (1996)	48			203-318	0.346-0.381	0.766
R-32/125/134a — Sound Speed						
Hozumi (1996)	27	0.0445-0.536		303-343	0.340	0.016
Hurly <i>et al.</i> (1997)	361	0.0512-0.982		260-400	0.346	0.00899
R-125/134a/143a — $p\rho T$						
Fujiwara <i>et al.</i> (1998)	162	1.5-15	0.481-12.7	263-403	0.357	0.3
Kleemiss (1997)	196	1.39-17.1	6.14-13.4	243-373	0.340	0.034
R-125/134a/143a — VLE						
Kleemiss (1997)	26	0.0698-3.15		223-344	0.316-0.331	0.246
Nagel and Bier (1995)	13	0.0167-3.96		204-363	0.159-0.171	0.577
R-125/134a/143a — Isobaric Heat Capacity						
Gunther and Steimle (1996)	24			203-318	0.357	1.68

^aAverage absolute deviation in density for p - ρ - T data and in bubble point pressure for VLE data. For second virial coefficients, numbers given are average absolute differences (cm³/mol)

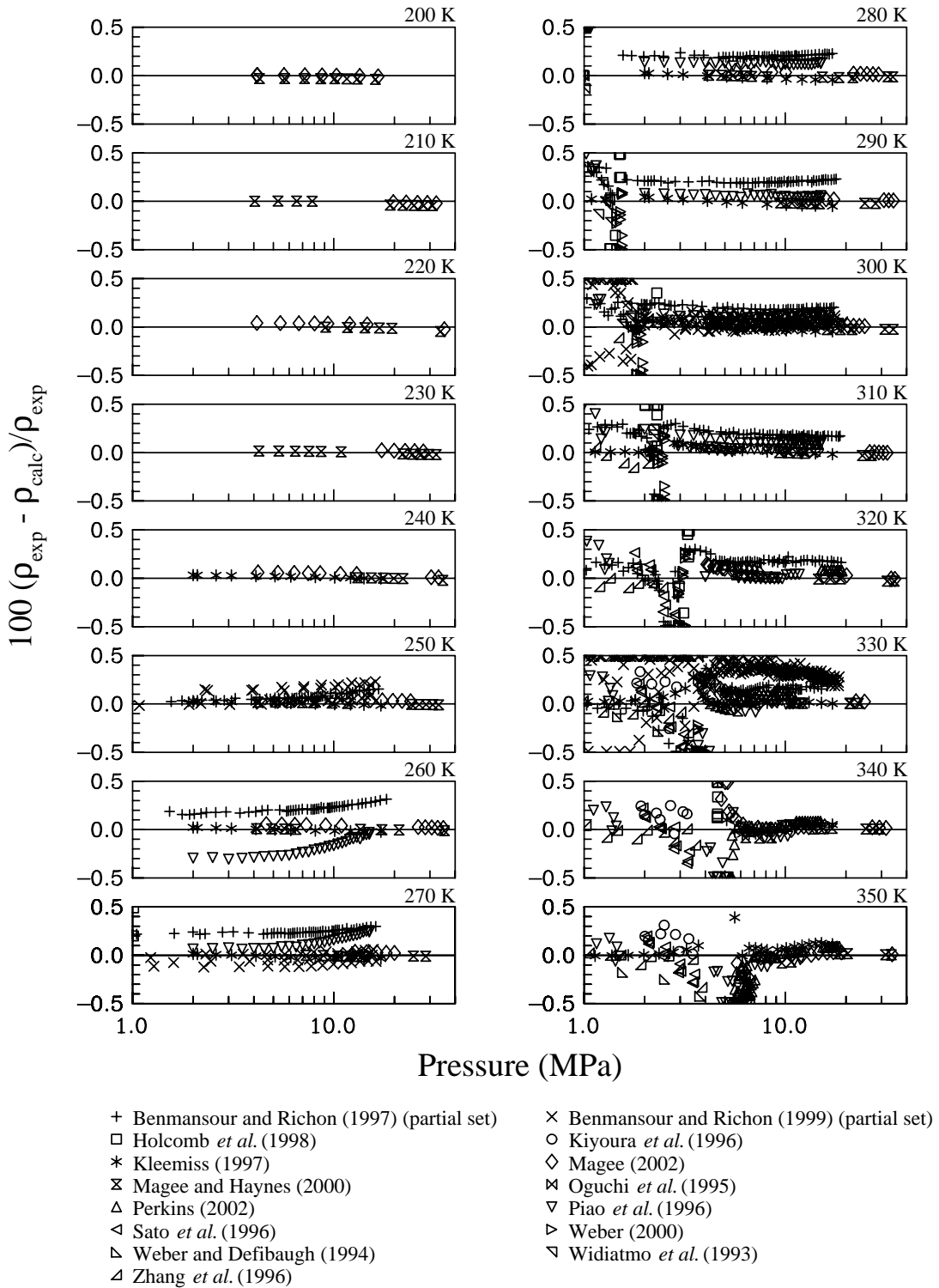


Figure 1. Comparisons of densities calculated with the mixture model to experimental data for the R-32/125 binary mixture.

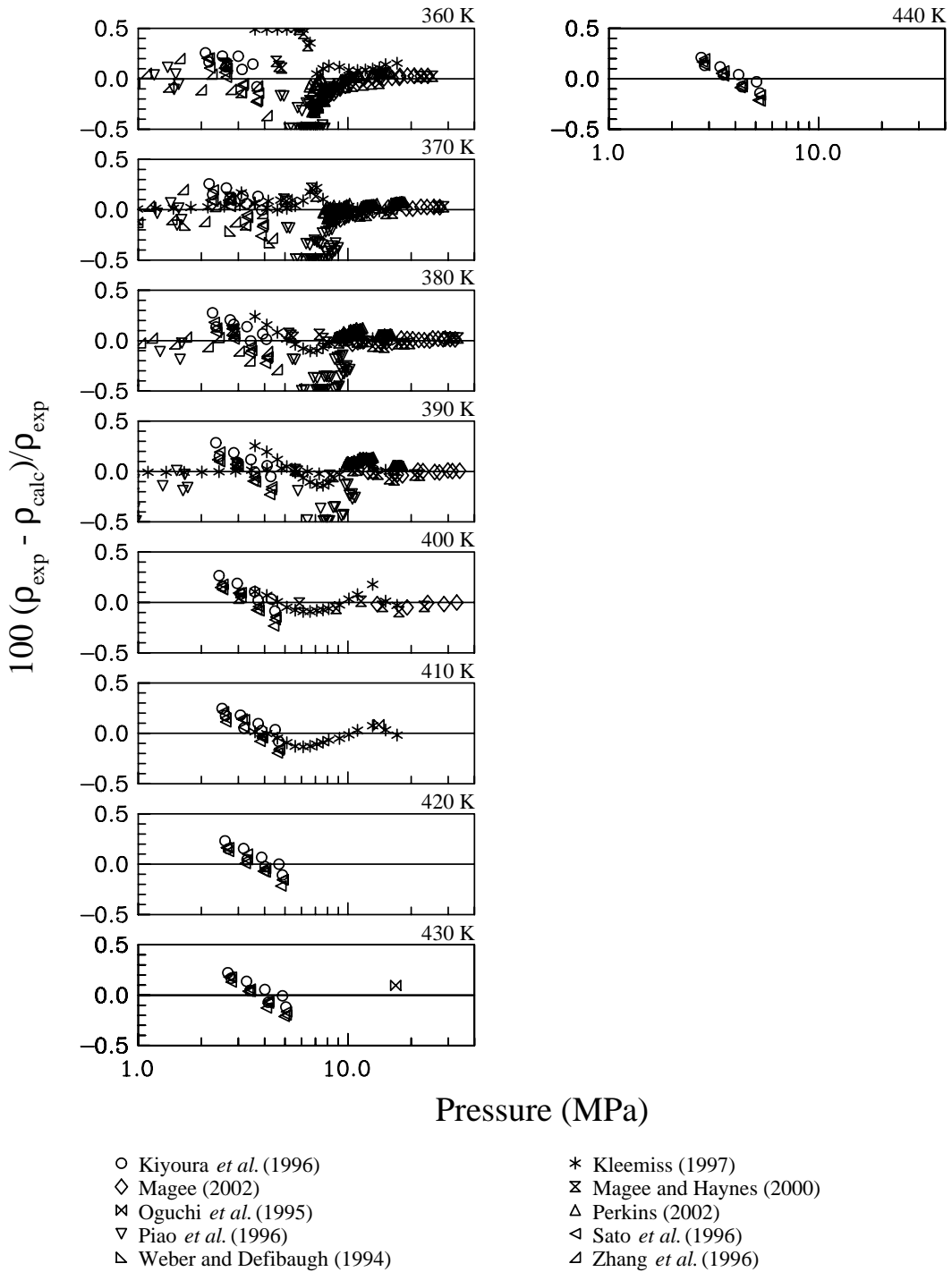


Figure 1. Comparisons of densities calculated with the mixture model to experimental data for the R-32/125 binary mixture (continued)

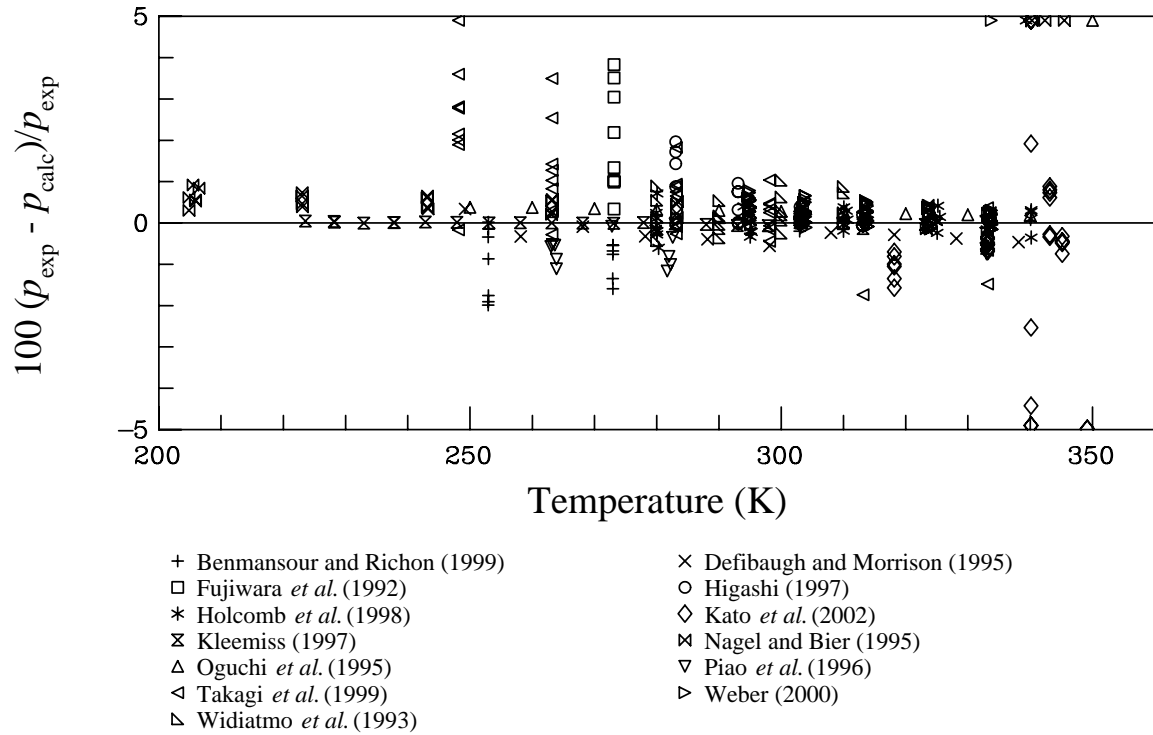


Figure 2. Comparisons of bubble point pressures calculated with the mixture model to experimental data for the R-32/125 binary mixture.

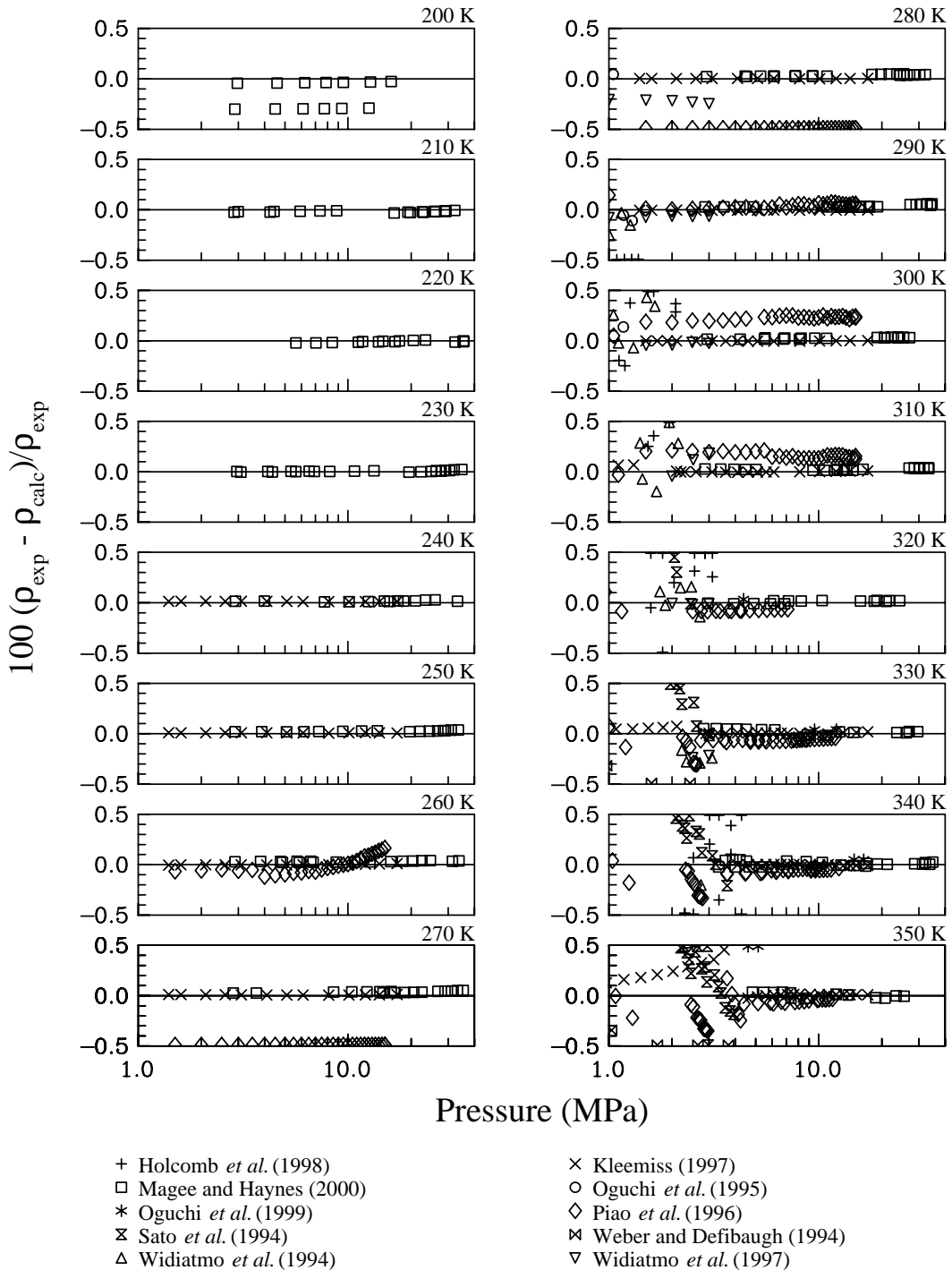


Figure 3. Comparisons of densities calculated with the mixture model to experimental data for the R-32/134a binary mixture.

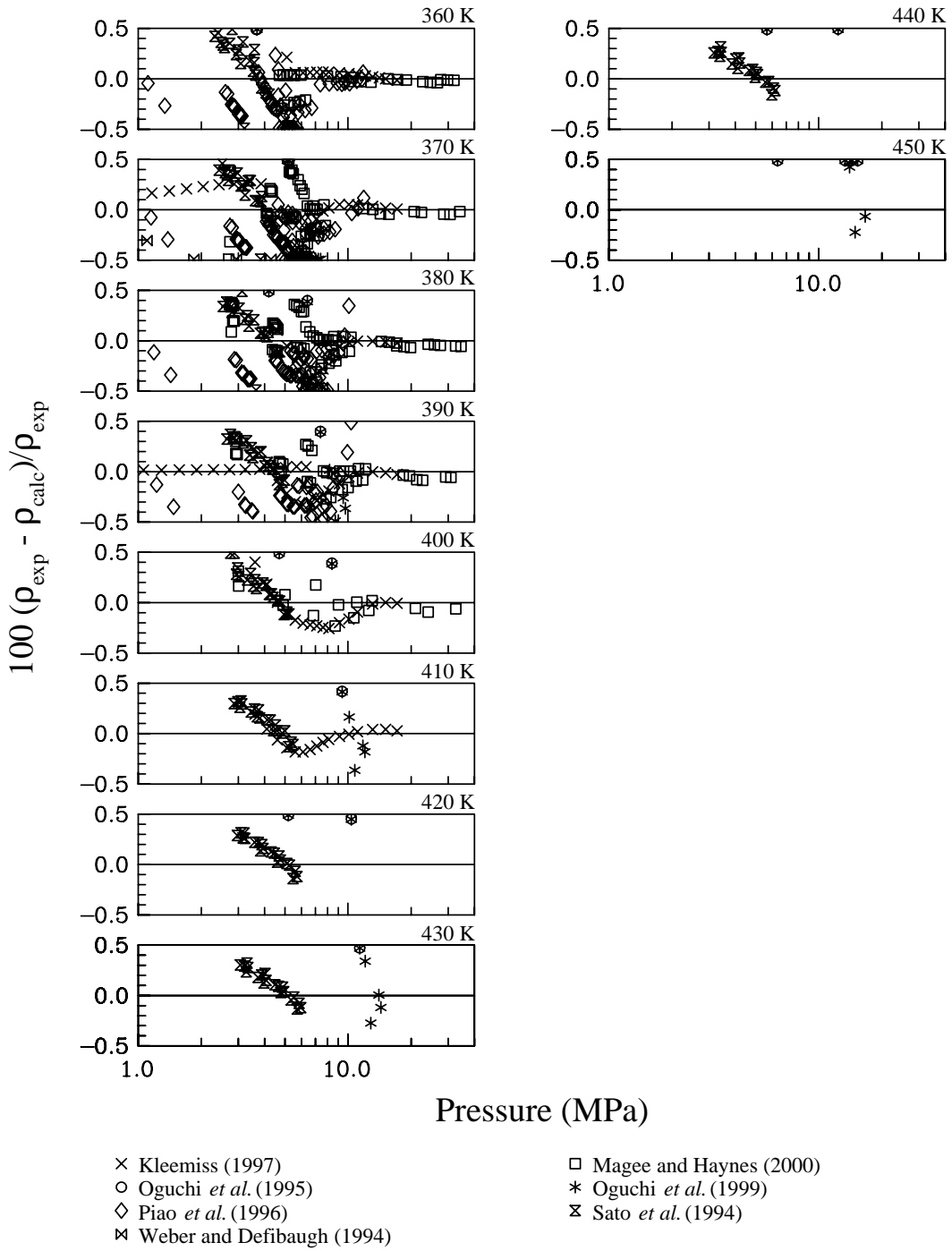


Figure 3. Comparisons of densities calculated with the mixture model to experimental data for the R-32/134a binary mixture (continued).

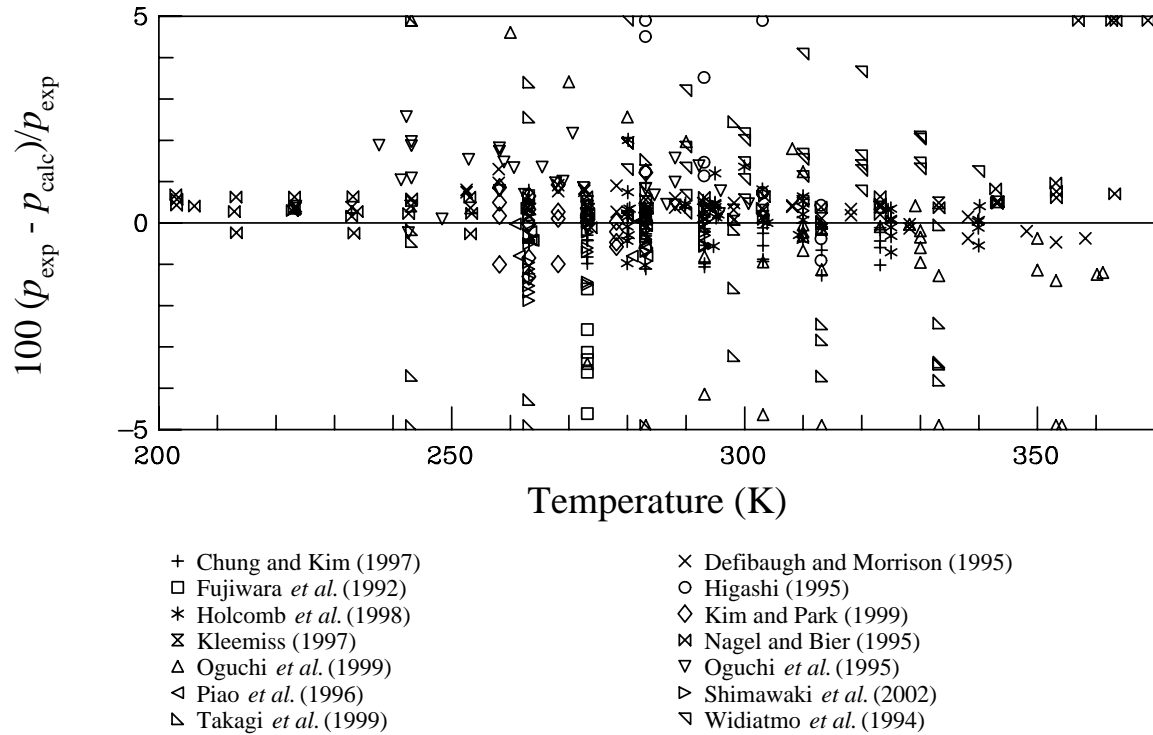


Figure 4. Comparisons of bubble point pressures calculated with the mixture model to experimental data for the R-32/134a binary mixture.

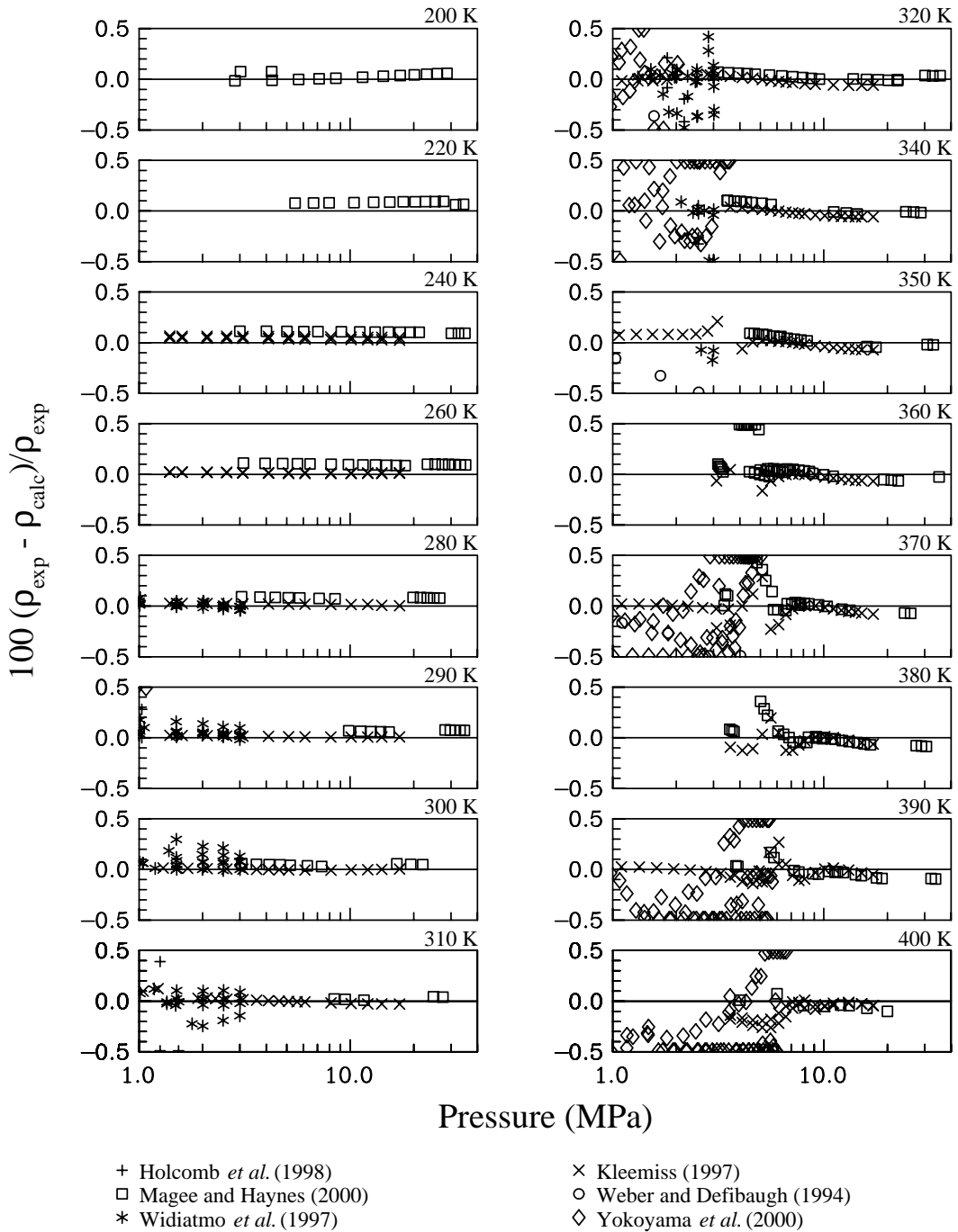


Figure 5. Comparisons of densities calculated with the mixture model to experimental data for the R-125/134a binary mixture.

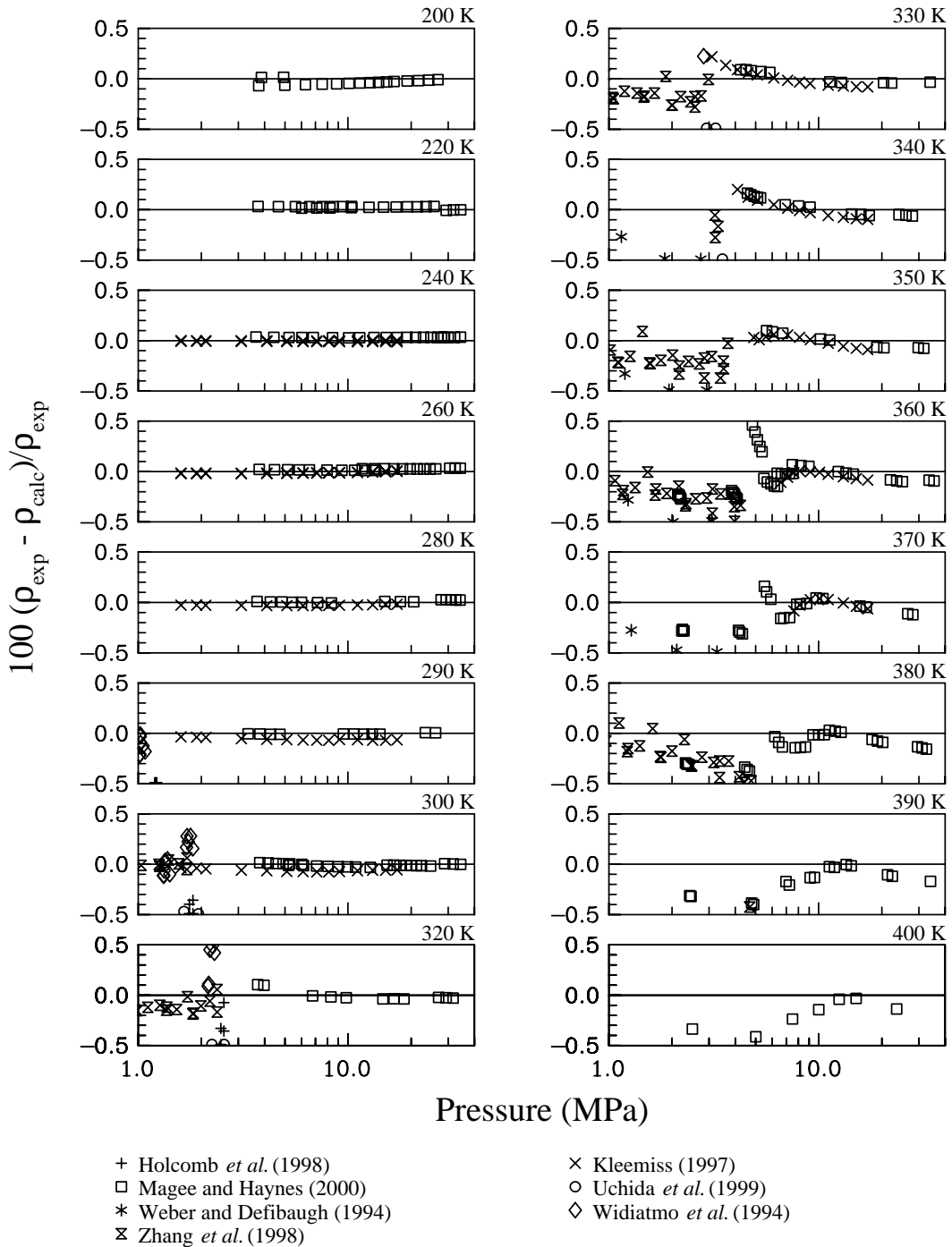


Figure 6. Comparisons of densities calculated with the mixture model to experimental data for the R-125/143a binary mixture.

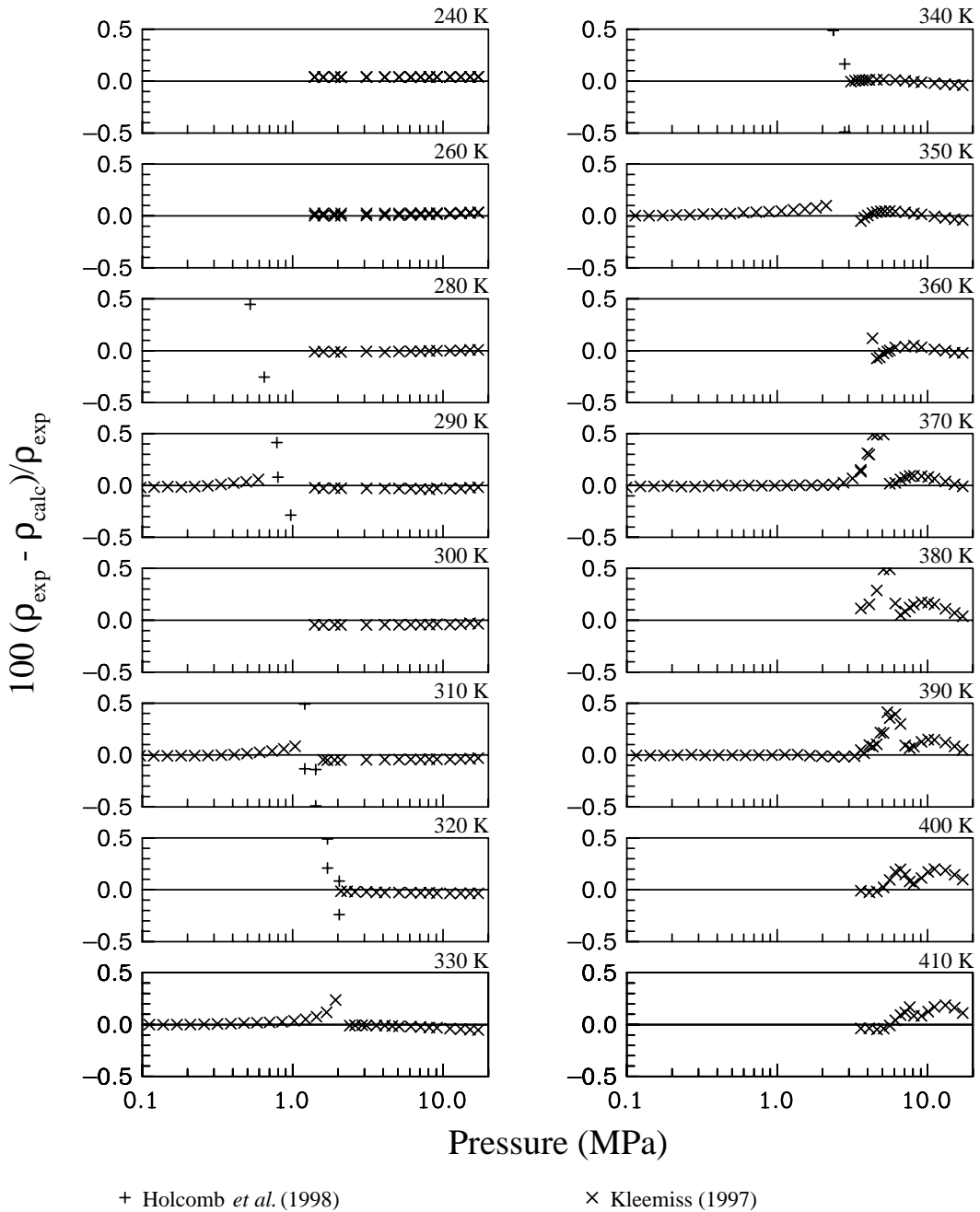


Figure 7. Comparisons of densities calculated with the mixture model to experimental data for the R-134a/143a binary mixture.

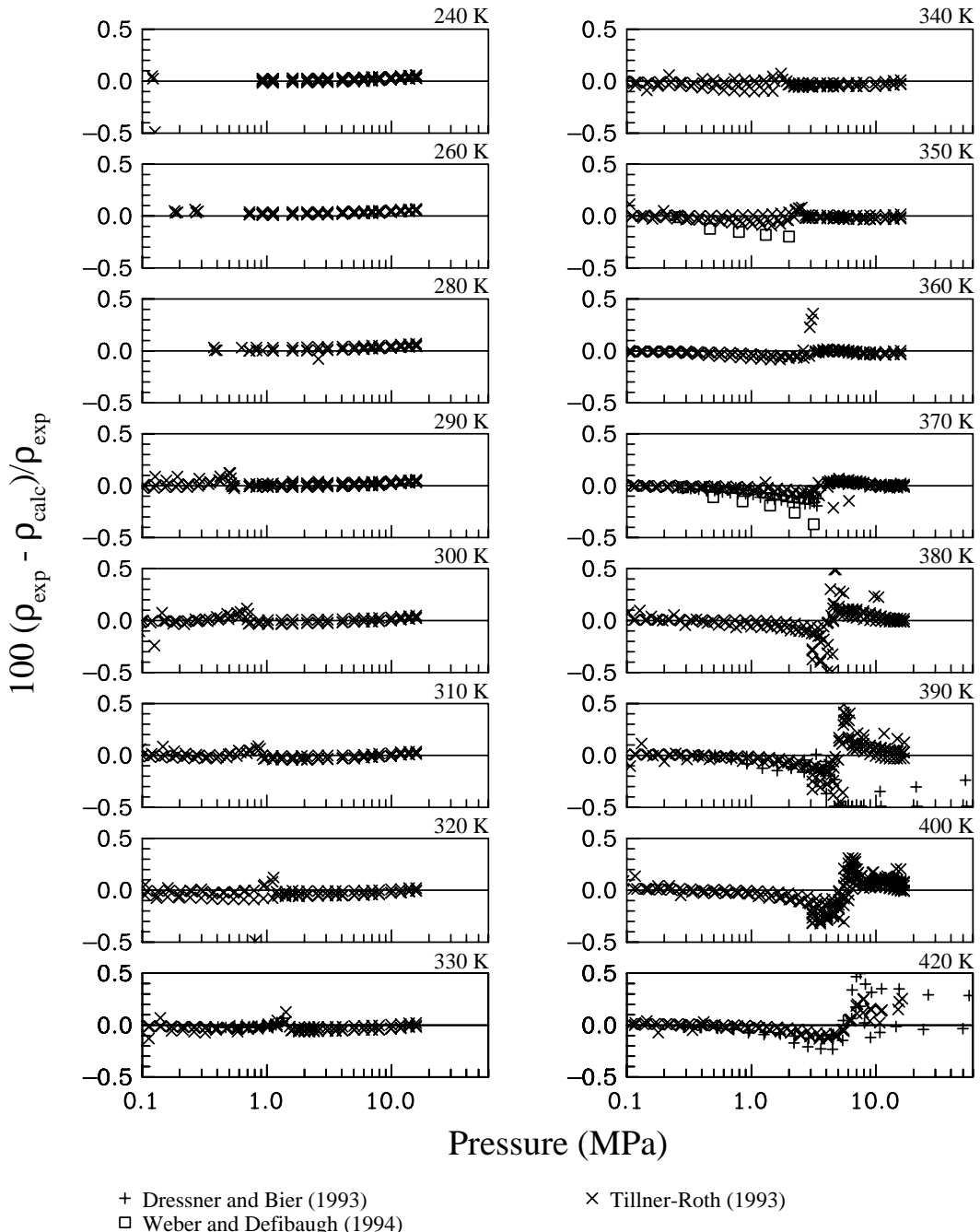


Figure 8. Comparisons of densities calculated with the mixture model to experimental data for the R-134a/152a binary mixture.

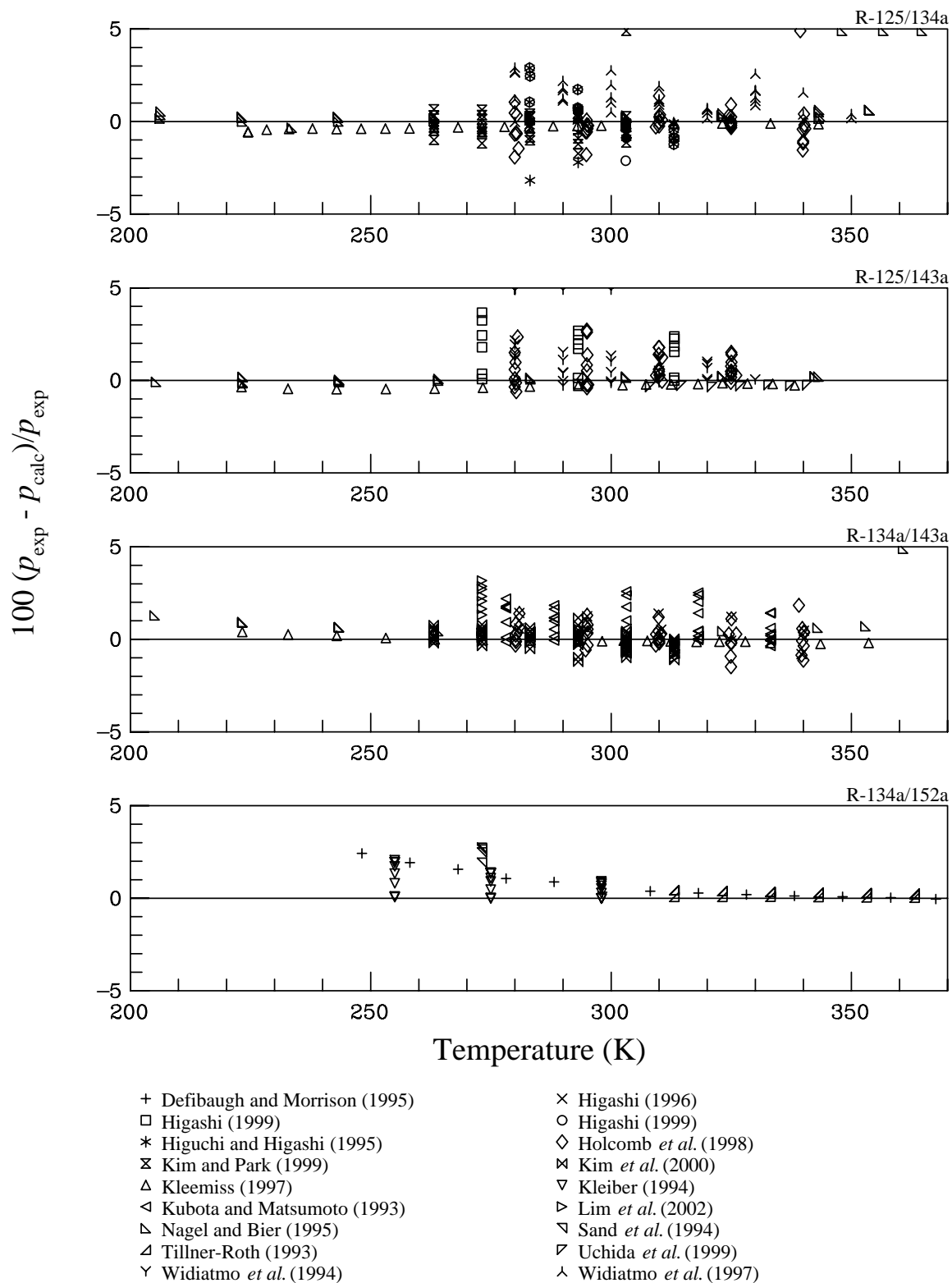


Figure 9. Comparisons of bubble point pressures calculated with the mixture model to experimental data for the R-125/134a, R-125/143a, R-134a/143a, and R-134a/152a binary mixtures.

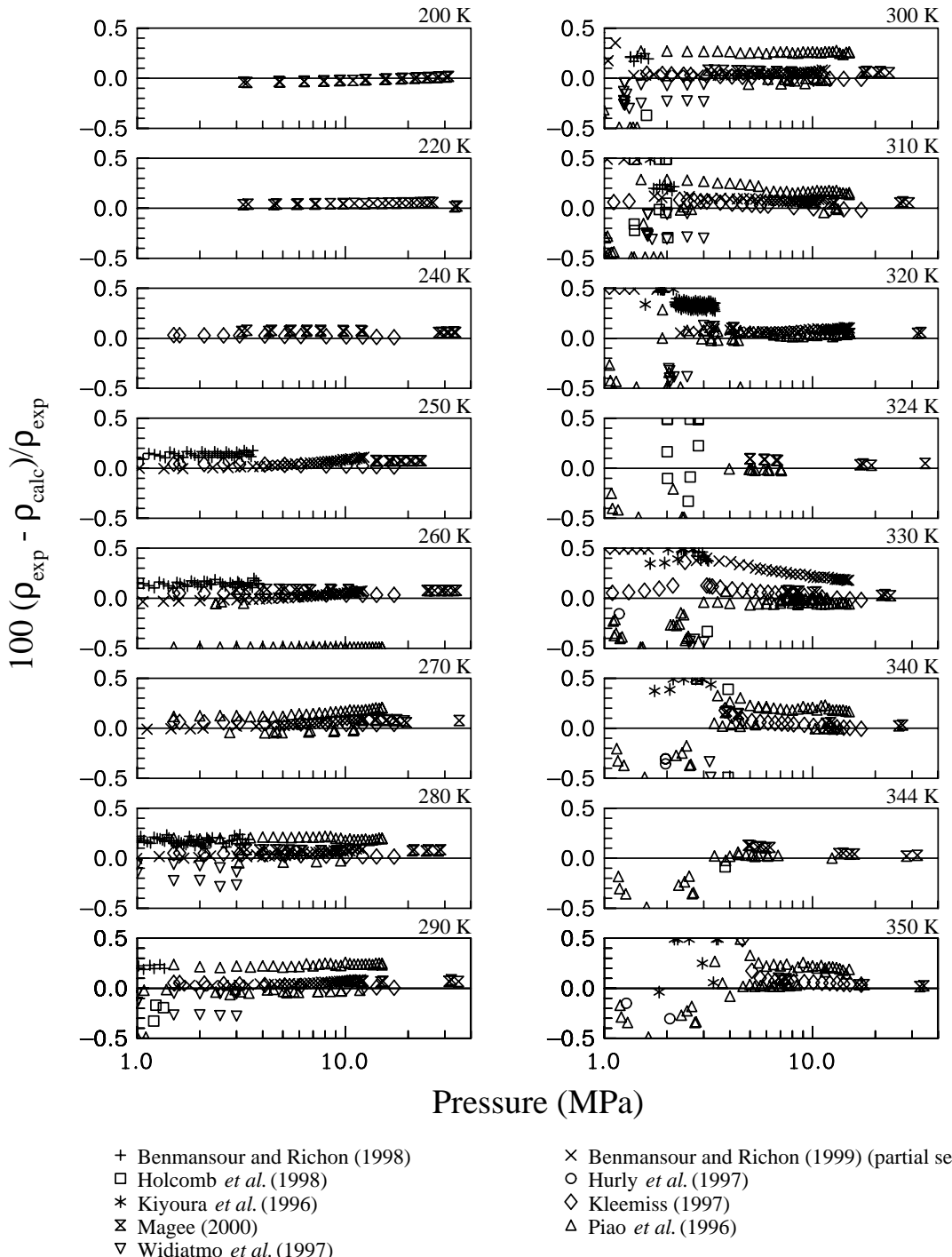


Figure 10. Comparisons of densities calculated with the mixture model to experimental data for the R-32/125/134a ternary mixture.

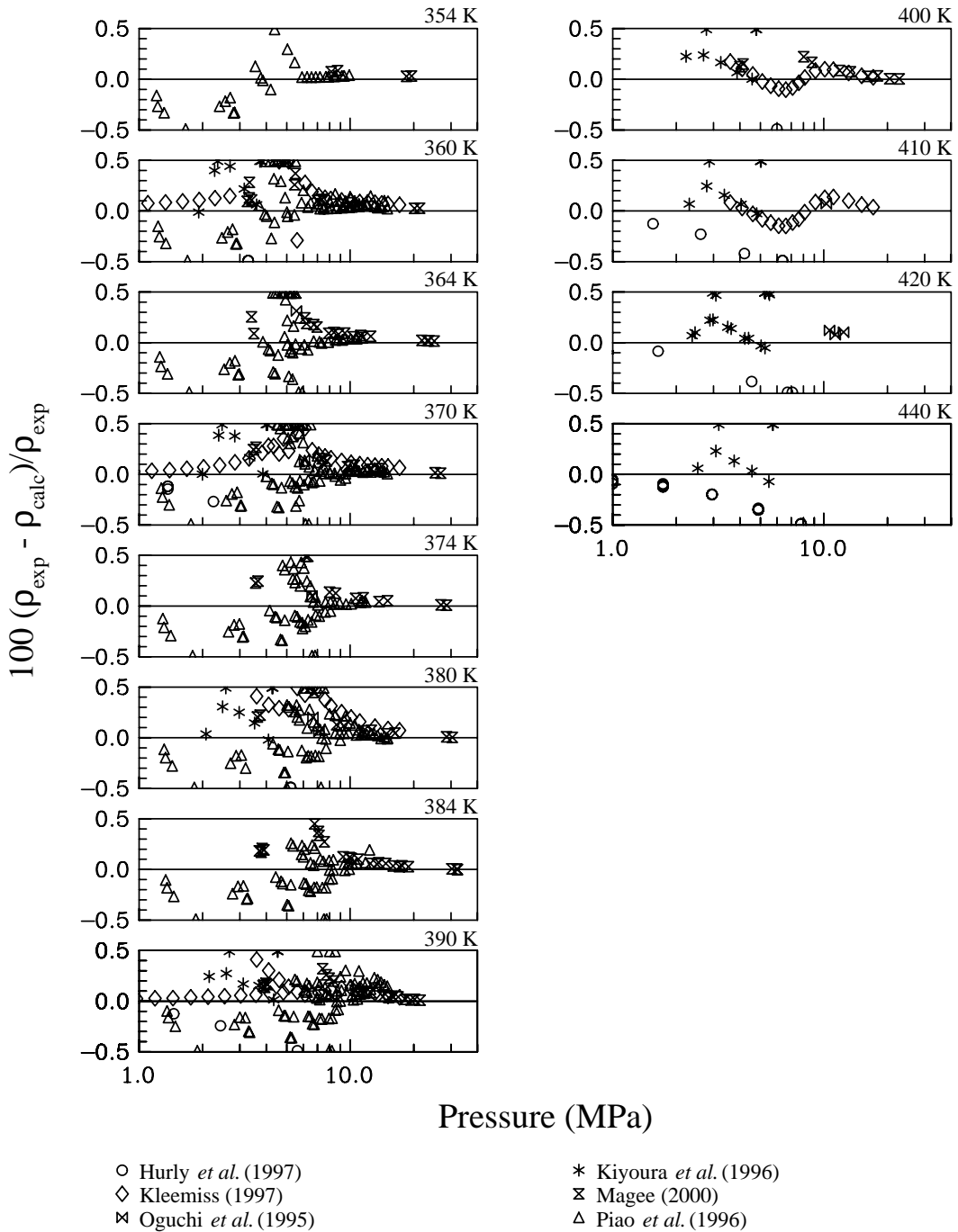


Figure 10. Comparisons of densities calculated with the mixture model to experimental data for the R-32/125/134a ternary mixture (continued).

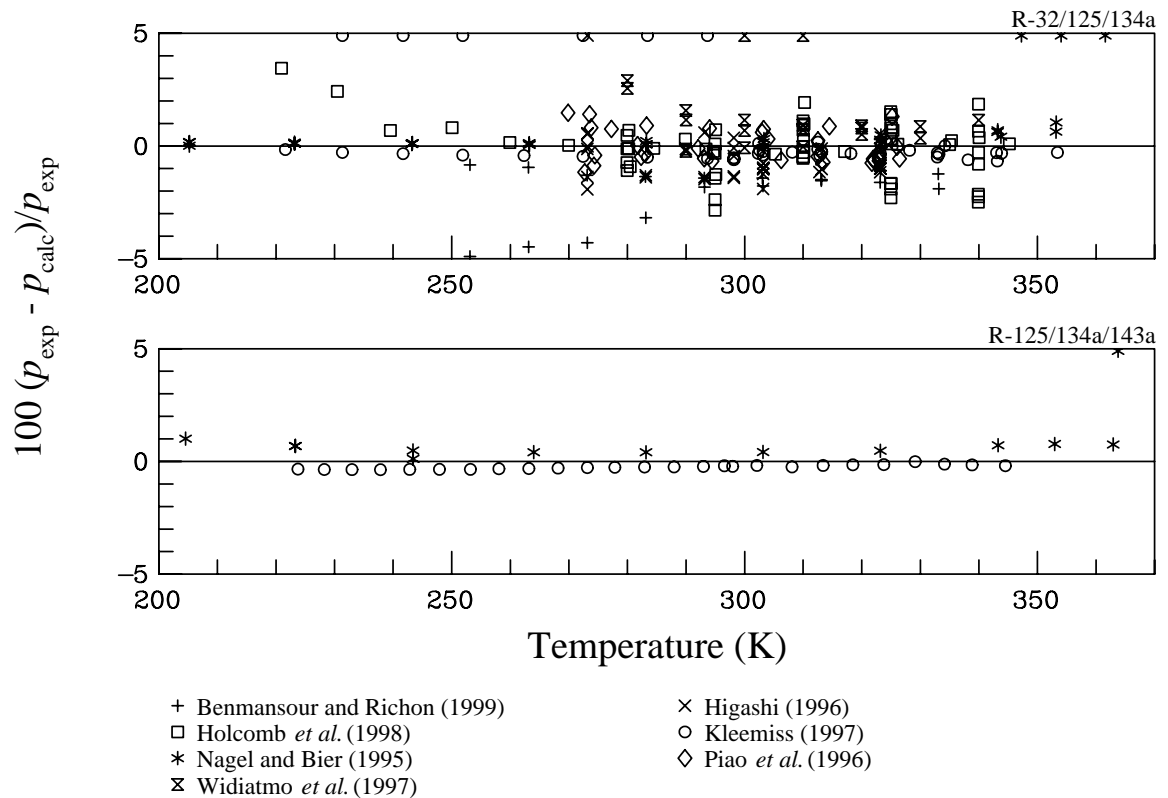


Figure 11. Comparisons of bubble point pressures calculated with the mixture model to experimental data for the R-32/125/134a and R-125/134a/143a ternary mixtures.

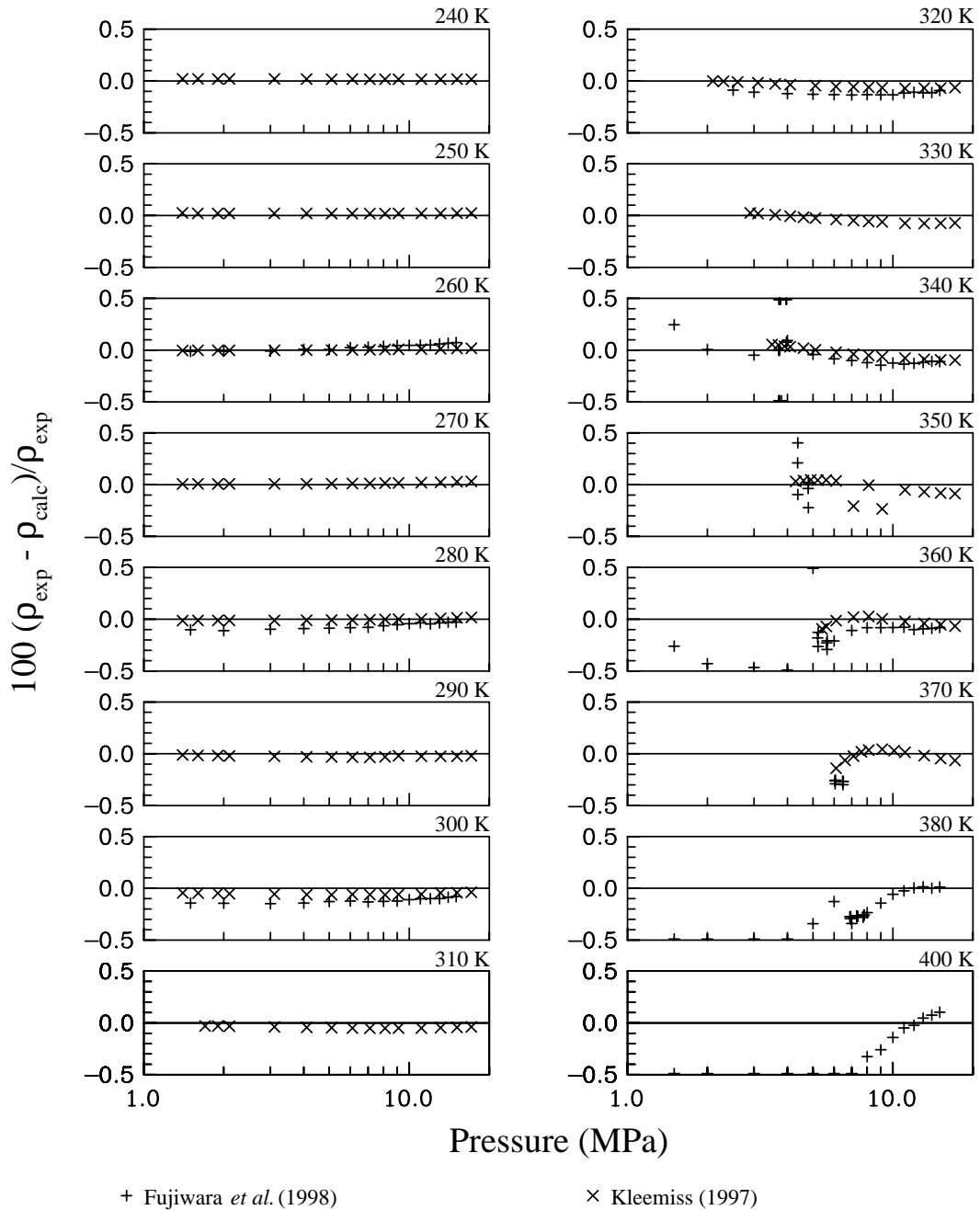


Figure 12. Comparisons of densities calculated with the mixture model to experimental data for the R-125/134a/143a ternary mixture.

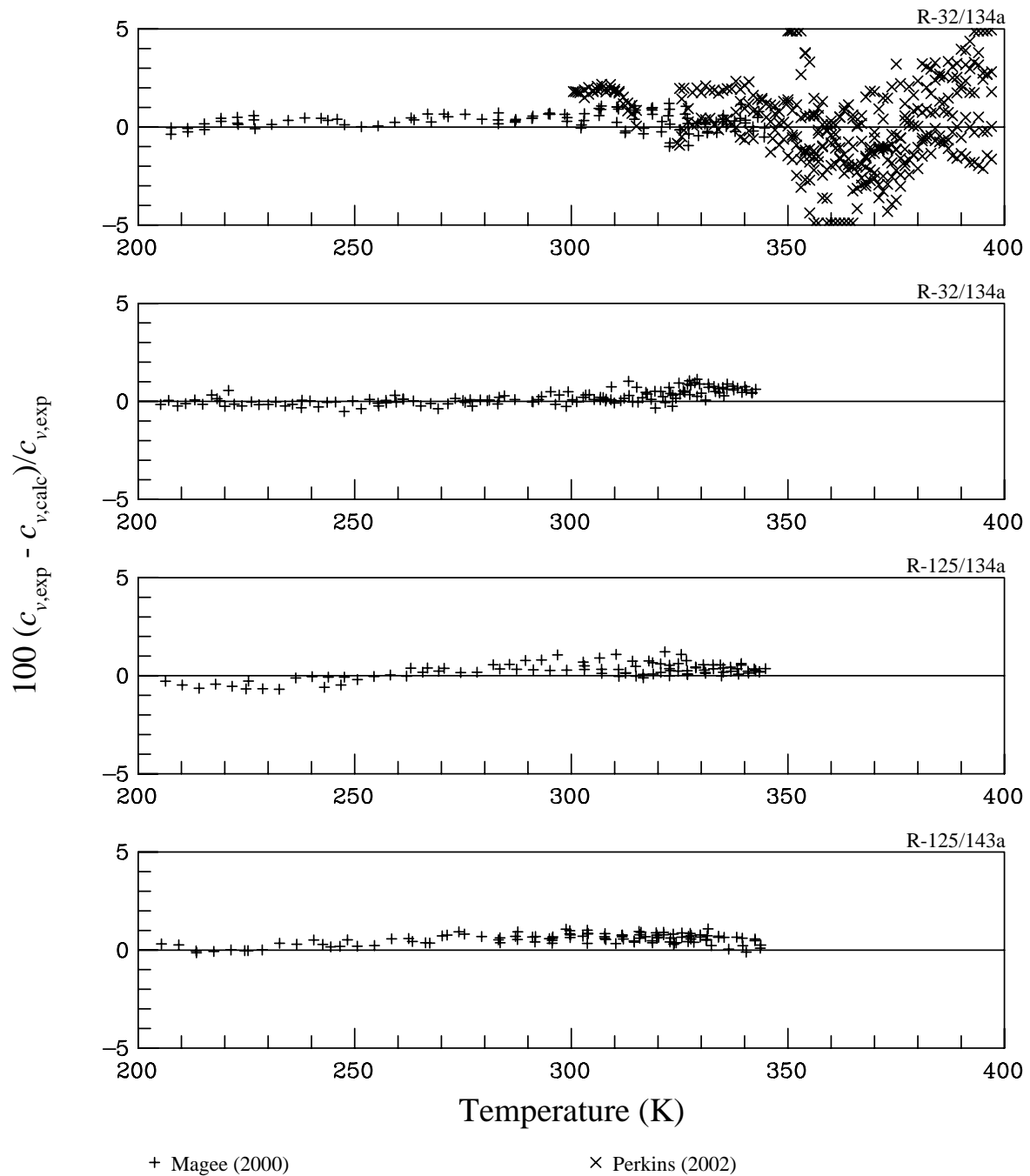


Figure 13. Comparisons of isochoric heat capacities calculated with the mixture model to experimental data for the R-32/125, R-32/134a, R-125/134a, and R-125/143a binary mixtures.

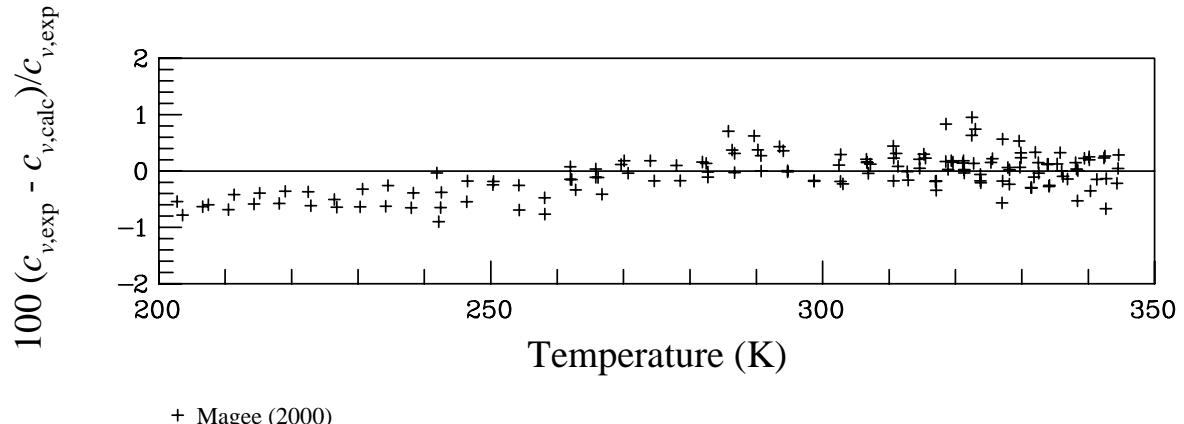


Figure 14. Comparisons of isochoric heat capacities calculated with the mixture model to experimental data for the R-32/125/134a ternary mixture.

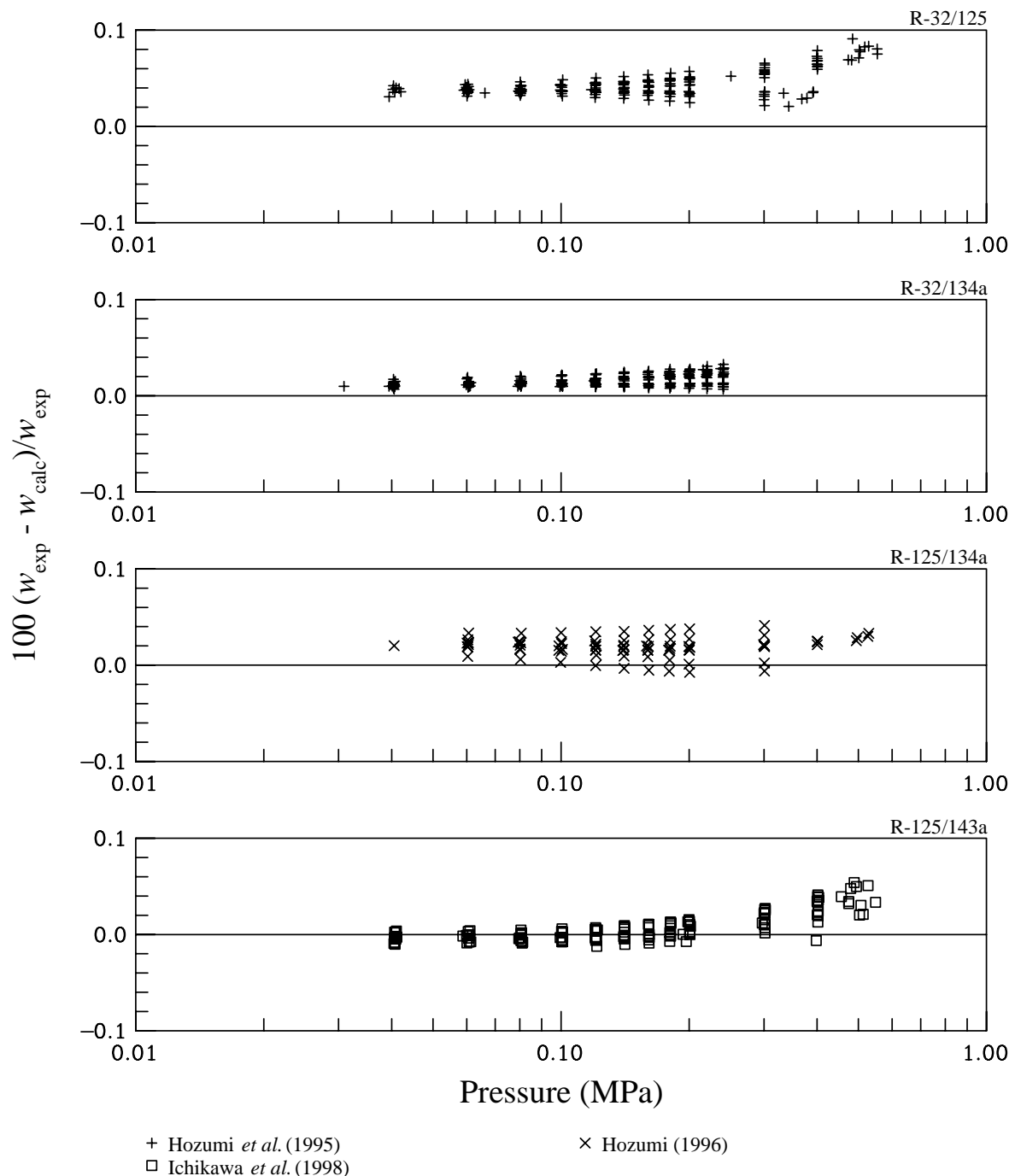


Figure 15. Comparisons of the speed of sound in the vapor phase calculated with the mixture model to experimental data for the R-32/125, R-32/134a, R-125/134a, and R-125/143a binary mixtures.

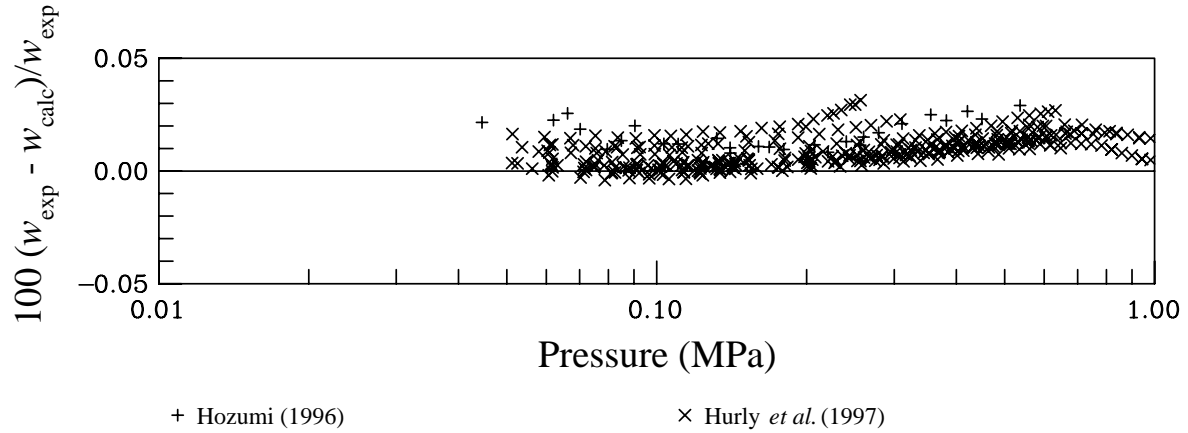


Figure 16. Comparisons of the speed of sound in the vapor phase calculated with the mixture model to experimental data for the R-32/125/134a ternary mixture.

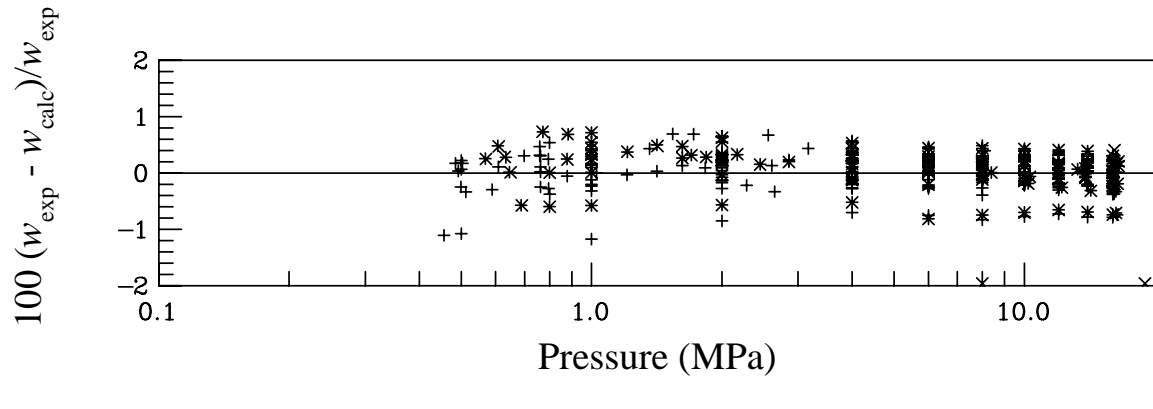


Figure 17. Comparisons of the speed of sound in the liquid phase calculated with the mixture model to experimental data for the R-134a/152a binary mixture.